Dynamic rating of HV/MV power transformers and effects on substation capacity

Exploring the limits and effects of transformer loading

Ramp, Alexander W.

Award date:
2023

Dynamic rating of HV/MV power transformers and effects on substation capacity

Exploring the limits and effects of transformer loading

by

Alexander Ramp

to obtain the degree of Master of Science
at the Eindhoven University of Technology,
to be defended publicly on Friday the 25th of August, 2023 at 10:00.

Student name	Student number
A.W. Ramp	1387480

Thesis supervisor:	dr. ir. J. Morren
Company supervisor:	T. van Cuijk
Project duration:	October, 2022 - August, 2023
Section, department:	Electrical Energy Systems, Electrical Engineering
Master's program:	Sustainable Energy Technology
Study load:	45 EC

TU/e

Summary

The energy transition is increasing the demand for electrical capacity. This demand is currently growing faster than the grid operators can supply through strengthening of the grid. Demand of grid capacity outpacing the supply places the majority of the Netherlands under congestion, unable to obtain additional grid connection capacity.

Faced with this dilemma, power system operators are exploring possibilities to cope with congestion in their substations. Congestion management was a possibility which is now implemented. It uses the flexibility of the energy system and combines it with an energy market. Through this energy market, grid system operators can buy a reduction in generation or demand to cope with congestion.

Using primary components more efficiently by applying dynamic rating is considered another possibility in this research. This dynamic rating stems from a components' thermal capacity under dynamic conditions. Additionally, if a primary component is the limiting factor of a substation, application of dynamic rating could provide additional electrical capacity.

This research focuses on substations which transfer power from the high voltage to the medium voltage network. One of the components in these stations with potential dynamic rating is the power transformer. The rating of these transformers is limited by maximum temperatures of its materials. To model these temperatures, the loading guide presents mathematical models derived from thermodynamics. These models are used to simulate a power transformer's dynamic rating. Using a load profile and ambient temperature as input, the model can calculate transformer temperatures and loss-of-life. This loss-of-life can be interpreted as additional depreciation costs, which can be compared with congestion management costs.

To validate the model and improve its accuracy it is applied to cases containing measured temperatures. The improved model is then applied under scenarios where the transformer is loaded above its nominal rating. These overloading scenarios result in costs due to additional depreciation and congestion management. By comparing both costs, the most cost-effective strategy for coping with overloading is identified.

This research concludes that a transformer's dynamic rating can be used to increase a substation's capacity, though the transformer has to be the limiting component. Furthermore, a transformer can be loaded above nominal rating, depending on the characteristics of the load. Lastly, in a comparison between costs of additional depreciation and congestion management, it was determined additional depreciation are more cost effective in overload scenarios compared to congestion management.

Contents

1

Introduction

In the Netherlands, the demand for electrical capacity is exceeding the current power grid capacity. Netbeheer Nederland, a branch organisation for the Dutch network operators, studied the growth in electrical capacity demand for different scenarios of the energy transition. This study projects the demand for electrical capacity will grow between 180% and 250% by 2050, compared to 2019 [1]. Multiple areas of the Netherlands currently have reached power grid capacity limits, both in demand and generation of electricity [2, 3], as can be seen in figure 1.1. As these limits are reached and demand for electrical capacity continues to grow, at least until 2050, it can be concluded that demand for electrical capacity is exceeding the current grid capacity.

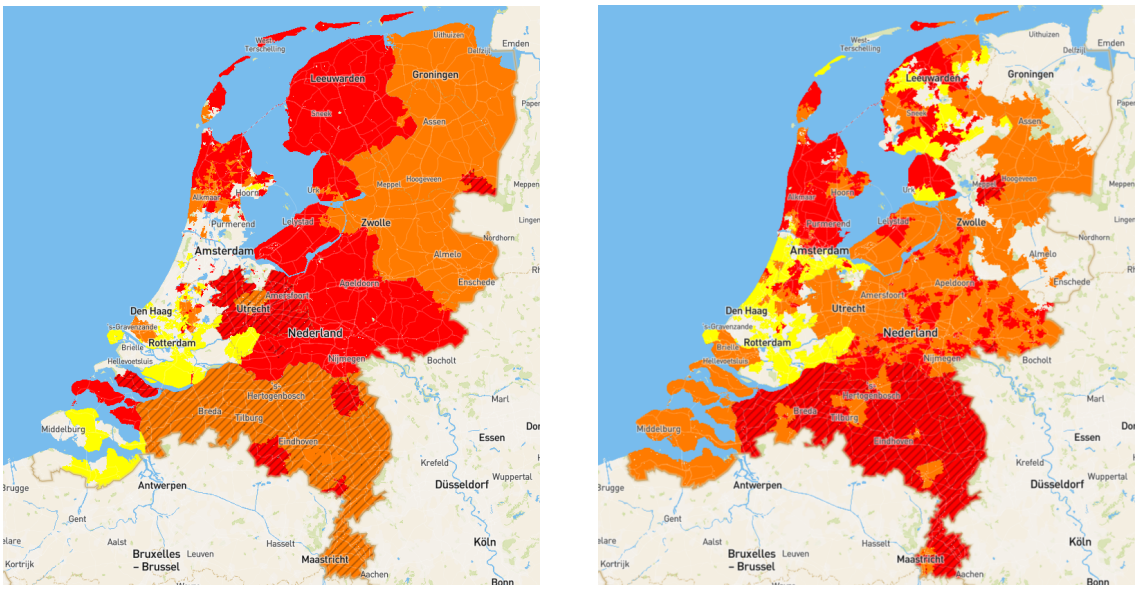

(a) (b)

Figure 1.1: Congested areas in the Netherlands for (a) electrical generation and (b) electrical demand. Yellow = looming scarcity of transport capacity, orange = announced structural congestion, red = structural congestion [3].

System operators are not able to expand grid capacity fast enough to keep up with growing capacity demand. The conventional method for increasing grid capacity is by strengthening the grid through expansion, replacement or a combination of both. A consortium of stakeholders in the Dutch energy system presented a plan to tackle the shortage of capacity, which is called congestion. In the plan, the consortium calls for a power grid which has to be strengthened to two or three times its current capacity in the next decade [4]. However, it also addresses the shortage of personnel needed by the Transmission System Operator (TSO) and Distribution System Operator (DSO) to achieve this grid strength,

which is a known problem [5]. Due to this shortage of personnel and the substantial grid strengthening needed, it can be said the rate of increasing capacity needed to relieve congestion is not feasible.

TSOs and DSOs are developing solutions which can alleviate congestion. One of the concepts which can alleviate congestion is called congestion management (CM). This concept uses the flexibility of the energy system to reduce load or generation exceeding the power grid capacity. Cable pooling and countering are options to shorten the waiting list of requests for additional capacity [6, 7]. Congested areas have an excess of requests for additional capacity, resulting in a waiting list. This waiting list impedes with customers' plans for expansion or sustainability. In cable pooling and countering, the customer can add generation or demand to their connection without increasing contracted capacity. Not having to increase contracted capacity can potentially shorten the waiting list for additional capacity and alleviate congestion.

Another concept which could contribute to alleviating congestion is more efficiently using the power grid components. A station's capacity is mainly determined by the rating of its components. This rating is the highest amount of current allowed to flow through a component at nominal voltage. The rating is determined by the component's manufacturer and is usually based on steady-state conditions such as constant loading and ambient temperature. By considering such conditions as changing over time, the rating of components becomes dynamic. This dynamic rating could potentially be higher or lower than the static rating. By using this dynamic rating, rather than static rating, the component could be used more efficiently. If the component is limiting the station's capacity, dynamic rating could potentially raise this capacity.

The effects of using dynamic rating in congestion management scenarios introduce a cost consideration effect. During congestion management scenarios, the excess load is re-dispatched on the costs of the DSO. These costs could be mitigated by accepting the excess load and overloading the limiting component, using its dynamic rating. However, this overloading is a risk as it can cause component failures or additional ageing, resulting in costs. The costs of congestion management and overloading components in the same scenario can be considered, introducing the cost consideration effect.

1.1. Research questions

From this context, the following research question is derived:

Can dynamic rating of power grid components provide additional capacity and what are the effects of applying said dynamic rating under congestion management scenarios?

This main research question is divided into the following sub-questions:

- What is the dynamic rating of power grid components?
- Which components affect capacity of substations?
- How does dynamic rating affect congestion management scenarios?
- How can the dynamic rating of components be modeled?
- What substations can be modeled using dynamic rating?
- What are the techno-economic effects of applying dynamic rating?

1.2. Scope

To limit the scale of the research a scope is determined. This research:

- is limited to HV/MV level substations of a DSO;
- is limited to power transformers;
- is limited to thermal capacity of transformers;
- does not consider power quality;
- does not consider failure rate and its effects.

The remainder of this report presents the research in the following manner: first, relevant components and their potential dynamic rating are identified; second, a method is presented to model thermal capacity of power transformers; third, results of the method are presented and analyzed; last, results are discussed and conclusions are given.

2

Rating of a substation's primary components

2.1. Substations

The distribution grid starts in the substations where High Voltage (HV) is transformed into Medium Voltage (MV), designated as HV/MV stations in this research. The DSO takes over grid responsibility from the TSO at the point where the transformer is connected to the HV transmission system. From this point, the electrical energy is transferred to the MV distribution system. The energy is then spread through the distribution system using multiple components such as cables, busbars, and switchgear.

HV/MV stations can currently be considered as the limiting factor in electrical capacity of an area. HV/MV stations supply energy to multiple distribution stations over a certain area. A characteristic of distribution stations is the similarity in load profiles of its connections. The distribution station distributes electrical energy to areas where the demographic tends to be similar. To cope with this larger similarity, substations are usually outfitted with more capacity than needed. This similarity is of less concern in HV/MV stations as it supplies more connections and thereby a larger demographic. Due to this phenomena, the capacity of an HV/MV station tends to be lower than the combined capacity of the substations it supplies. This tendency is why HV/MV stations can be considered the limiting factor in capacity of an area.

The scope presented in chapter 1 mentions HV/MV stations as the focus of this research. The preceding paragraph argues why these stations are the limiting factor in electrical capacity of an area. Additionally, congestion is mainly caused by HV/MV stations as shown by the congestion investigations of Enexis [8]. As the HV/MV stations can be considered limiting and are main causes of congestion, they are the focus of this research.

2.2. Substation primary components

A substation's components can be divided in three categories; primary, secondary and tertiary. Primary components conduct the electricity which is transported through the power system such as transformers, cables and switchgear. Secondary components provide ancillary services to the grid such as communication, measurements, control and system protection. Tertiary components provide functions such as safety and security in the form of enclosures or casings in which primary and secondary components can be mounted.

2.3. Rating of primary components

The rating of an electrical component is generally limited by the thermal properties of its materials. Power flow through a component introduces a heat source due to resistance losses. If this heat source causes a surplus in a component's thermodynamic balance, its temperature increases [9]. These in-

creases can change material properties and may cause failures of components, resulting in faults or short-circuits. Due to these risks, a components' rating is generally based on temperature limits.

2.4. Overloading of components

Some components can be overloaded relative to their static rating due to the dynamics of their thermal capacity. Components have a thermal capacity based on their mass and material properties [9]. Energy can be stored in a system's internal capacity, raising the temperature. The rate of temperature change due to change in internal energy is related to its time constant. This time constant acts as an inertia in the temperature response to load changes. Additionally, component ratings are usually based on steady state conditions. One of these conditions is the constant loading of the component. However, the loading of a component in practice is dynamic. Due to this dynamic loading, the component can be shortly loaded above nominal rating until nominal conditions are reached. The inertia and dynamic loading can be used to shortly overload a component, as long as its temperature limits are not reached.

2.5. Power transformers

Power transformers in HV/MV stations are large and heavy objects. These characteristics are due to the amount of power they need to transfer. Generally, the mass and volume of a transformer increase with its rating. In the Netherlands, ratings of HV/MV transformers are usually in the tens of MVA. Recently, however, DSOs have started installing HV/MV transformers with ratings above 100 MVA.

The main components of a transformer are the laminated core, windings surrounding the core, the oil tank, cooling tubes and connection bushings. A graphical representation of a transformer and its components is presented in figure 2.1. The iron core is surrounded by copper windings and immersed in a tank full of oil. The oil provides dielectric strength and cooling to the core and windings. This cooling is achieved using the oil as a medium and the cooling tubes as heat exchanger with the ambient. This heat exchange can be natural or forced, through the use of ventilator or compressors. Usually HV/MV transformers are of the type Oil Natural Air Natural (ONAN) or Oil Natural Air Forced (ONAF). Due to their mass characteristic, HV/MV transformers have potential to be overloaded significantly using dynamic rating.

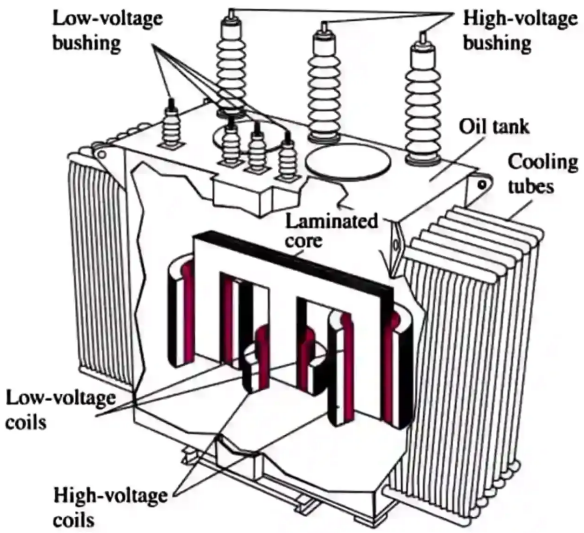

Figure 2.1: Graphical representation of a power transformer and its inner structure [10].

A transformer's lifetime is based on the deterioration of the paper insulation. The windings of a transformer are encapsulated with paper insulation. This insulation provides the dielectric strength between windings to prevent short-circuits and faults. As replacing the paper is more costly than buying a new transformer, the lifetime of a transformer is usually based on the life expectancy of the paper insulation.

3

Methods for modeling thermal capacity of power transformers

This chapter presents the methods used to model thermal capacity of power transformers. Furthermore, it presents a method to quantify the effects of applying dynamic rating in scenarios of loading above transformer nominal rating.

3.1. Transformer temperature model

The permissible (over)loading of power transformers is limited by its top-oil and winding hot-spot temperature limits. In their loading guide for mineral-oil-immersed power transformers, the International Electrotechnical Commission (IEC) presents maximum permissible temperature limits for the top-oil and winding hot-spot [11]. Figure 3.1 shows the location of the top-oil and the hot-spot temperature. The top oil is located on top of the windings, which is the location of the top-oil temperature θ_o. The hot-spot temperature rise $\Delta\theta_h$ is located at the point where the windings meet the paper insulation and is also the location of the hot-spot temperature θ_h.

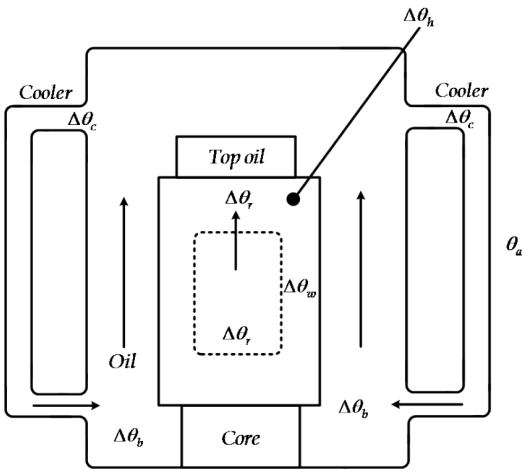

Figure 3.1: Cross-section of a power transformer and the locations of top-oil and hot-spot temperatures [12].

According to the loading guide, the temperature limits are specified for different categories: normal cyclic loading, long-term emergency loading and short-term emergency loading. This research uses the temperature limits for normal cyclic loading for two reasons. First, the intention of this research is to apply dynamic rating under normal operating conditions. Second, the limits for normal cycling loading are lowest, providing a safety margin. The top-oil and winding hot-spot temperature limits under normal

cyclic loading are 105 °C and 120 °C, respectively.

An electrical representation of a transformer is given in figure 3.2. The load factor K is the ratio between current of the load I_{load} and nominal current of the transformer I_{nom}, as determined in equation 3.1. In this research, the effects of the current's flow directions are assumed to be equal, meaning the absolute value of I_{load} is taken.

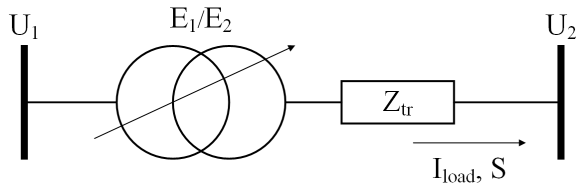

Figure 3.2: Electrical representation of a transformer

$$K = \frac{|I_{load}|}{I_{nom}} = \frac{S \cdot E_{ls}}{S_{nom} \cdot U_{ls}} \tag{3.1}$$

Top-oil and hot-spot temperatures can be calculated using mathematical models. The loading guide specifies differential equations for top-oil and hot-spot temperatures, θ_o and θ_h in equations 3.2 and 3.3. The inputs for these equations are load factor K, specified in equation 3.1, and ambient temperature θ_a.

$$\left[\frac{1 + K^2 \cdot R}{1 + R}\right]^x \cdot (\Delta\theta_{or}) = k_{11}\tau_o \cdot \frac{d\theta_o}{dt} + [\theta_o - \theta_a] \tag{3.2}$$

The hot-spot temperature is obtained by adding the top-oil temperature θ_o and hot-spot temperature change $\Delta\theta_h$ in equation 3.3.

$$\theta_h = \theta_o + \Delta\theta_h \tag{3.3}$$

The hot-spot temperature change is the change in winding temperature $\Delta\theta_{h1}$ due to load minus the temperature change due to the surrounding oil $\Delta\theta_{h2}$ as defined in equations 3.4, 3.5 and 3.6.

$$\Delta\theta_h = \Delta\theta_{h1} - \Delta\theta_{h2} \tag{3.4}$$

$$k_{21} \cdot K^y \cdot (\Delta\theta_{hr}) = k_{22} \cdot \tau_w \cdot \frac{d\Delta\theta_{h1}}{dt} + \Delta\theta_{h1} \tag{3.5}$$

$$(k_{21} - 1) \cdot K^y \cdot (\Delta\theta_{hr}) = (\tau_o / k_{22}) \cdot \frac{d\Delta\theta_{h2}}{dt} + \Delta\theta_{h2} \tag{3.6}$$

To calculate the top-oil and hot-spot temperatures over time, the differential equations are solved numerically using the Euler method. The process is assumed to be in steady state in the first step to obtain a solution at $t = 0$.

The differential equations contain constants which are presented in table 3.1. The table also presents standard values for these constants determined by the loading guide [11]. The constants $\Delta\theta_{hr}$, $\Delta\theta_{or}$ and R are specific per transformer and are taken from either the Factory Acceptance Test (FAT) or a recent heat run test report. Constant R is the short-circuit power divided by the no-load losses, according to equation 3.7.

$$R = \frac{P_{short-circuit}}{P_{loss}} \tag{3.7}$$

Parameter	ONAN	ONAF
Oil exponent x	0,8	0,8
Winding exponent y	1,3	1,3
Constant k_{11}	0,5	0,5
Constant k_{21}	2	2
Constant k_{22}	2	2
Oil time constant $\tau_o(min)$	210	150
Winding time constant $\tau_w(min)$	30	30

Table 3.1: Standard parameters for ONAN and ONAF power transformers as per the loading guide [11]

3.2. Transformer loss of lifetime due to overloading

Overloading of transformers causes additional loss of lifetime. The windings of transformers are insulated using paper insulation. This paper's ageing rate is a function of temperature as shown in equation 3.8 and is determined in the loading guide [11]. The equation determines the relative ageing rate V, which is an exponential function of the hot-spot temperature θ_h. The actual amount of ageing L is calculated over a time period $[t_n, t_{n+1}]$ using equation 3.9. In this research, the amount of ageing L of the paper insulation is assumed as additional ageing on top of the natural ageing of the transformer.

$$V = 2^{(\theta_h - 98)/6} \tag{3.8}$$

$$L = \int_{t_n}^{t_{n+1}} V \, dt \tag{3.9}$$

3.3. Validation & curve fitting

The measured top-oil and hot-spot temperatures presented in section 3.5 can be used to validate the model by checking its accuracy. The accuracy of the model is calculated using Mean Absolute Percentage Error (MAPE) and Root Mean Square Error (RMSE). The MAPE is the mean relative deviation between measured and simulated value and is convenient due to its expression in percentages. The RMSE is the root of the mean squared deviation between measured and simulated value and has the important characteristic of increased weighing of larger errors. The equations for the MAPE and RMSE are presented in equations 3.10 and 3.11, respectively. In the equations, A_t is the actual value measured, S_t is the simulated value and n is the total amount of time steps in the dataset.

$$MAPE = \frac{100\%}{n} \sum_{t=1}^{n} \left| \frac{A_t - S_t}{A_t} \right| \tag{3.10}$$

$$RMSE = \sqrt{\frac{\sum_{t=1}^{n} (A_t - S_t)^2}{n}} \tag{3.11}$$

To improve the accuracy of the model, it can be curve fitted. By creating sets of varying parameters out of table 3.1 and calculating the model accuracy using each parameter set, the optimal set of parameters can be found. This optimal set is, in theory, the set of parameters which result in the simulation with the highest accuracy. The accuracy metric used for this is the RMSE as the MAPE has a bias towards negative deviation [13].

Furthermore, the loading guide mentions model accuracy increases with loading of the transformer. In an effort to further increase accuracy, the MAPE and RMSE are calculated for peak loading values as well. The peak loading values are assumed to be the loads above one standard deviation of the mean of all loads. The accuracy of temperatures resulting from these loads are then used to determine whether accuracy increases with loading. The outcome of this peak accuracy is then considered in the curve fitting method.

This method is computationally intensive and time-consuming, as the model calculates results of the base case for every set of parameters. Therefore, the amount of parameters to optimize is reduced.

For top-oil temperature, parameters x and τ_o are curve fitted. For hot-spot temperature, parameters y and τ_w are curve fitted. These parameters are chosen based on research using sensitivity analyses to improve transformer thermal models [14, 15].

3.4. Comparing overloading and congestion management

3.4.1. Costs of overloading

A comparison can be made between transformer overloading and congestion management in terms of costs. Overloading transformers introduces additional ageing. This ageing can be expressed as additional depreciation costs. In this research the price of a new transformer is assumed to be two million euros and the depreciation lifetime is considered to be 50 years. When using linear depreciation, the costs per year of lifetime use can be determined using formula 3.12. Using this formula, the cost of additional depreciation due to overloading are assumed to be €100.000,- per year.

$$\text{cost per year of lifetime use} = \frac{\text{transformer price}}{\text{expected lifetime use}} = \frac{€2.000.000}{50} = \frac{€100.000}{year} \tag{3.12}$$

3.4.2. Congestion management

The introduction shortly described congestion management and its ability to relieve congestion. The concept is graphically illustrated in figure 3.3. Figure 3.3a presents a demand profile and figure 3.3b presents a generation profile. As can be seen, the load profiles exceed the capacity limit at certain time frames, marked by the hatched areas. These areas mark the amount of energy which has to be either re-dispatched or curtailed [16].

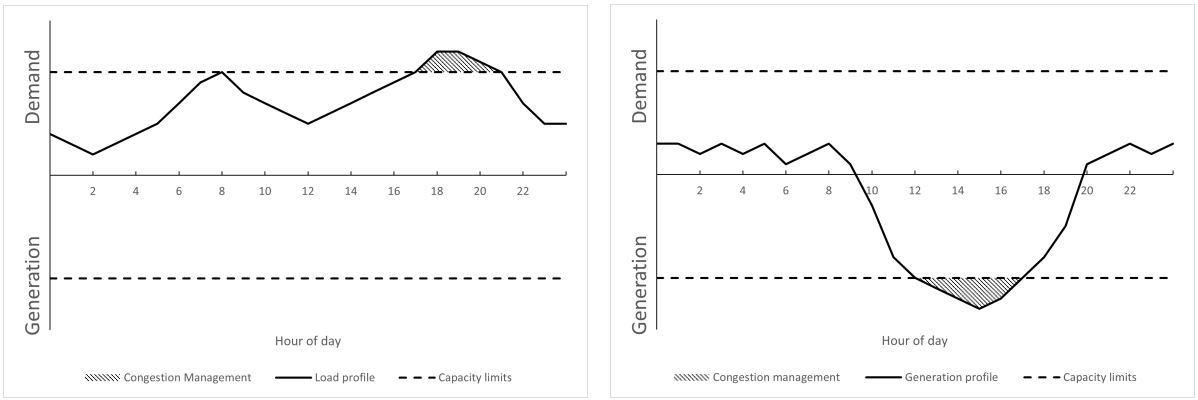

(a) **(b)**

Figure 3.3: A graphical representation of congestion management. In this case it is used to reduce demand when the load profile exceeds the capacity limit in figure 3.3a, or reduce generation when load profile exceeds the capacity limit in figure 3.3b

To determine the costs of congestion management, it is assumed that the nominal rating of the transformer is the threshold above which congestion management is applied. The surplus load above this threshold is re-dispatched so transformer load is limited at the threshold. Based on the total re-dispatch volume and price in 2022 on congestion management platform GOPACS [17], the re-dispatch costs are assumed to be €327,- per MWh. By calculating the costs of overloading and re-dispatching per case, the comparison between accepting additional depreciation and congestion management costs can be made.

3.5. Setup of modeled cases

Multiple cases are defined to model loading, top-oil and hot-spot temperature, and ageing for a single transformer. These cases are determined per HV/MV substation for the time period of 2022. Each substation has a base case and multiple overload cases. The base case consists of the actual transformer

loading of 2022 and includes measurements of top-oil and winding hot-spot temperatures. These temperatures are used to validate and curve fit the model.

The overload cases are constructed out of the base case by adding additional load. The load added to the base case is generated by a projection tool developed by Enexis engineers. The tool can create projections of the base case. A composition of load can then be added to this base case, to create an overload case. If the substation has a load primarily consisting of demand, a composition of electrical demand from the industrial, logistical and housing sector is added to achieve overloading. Similarly, if a substation has a load primarily consisting of generation, a composition of solar and wind generation is added to achieve overloading.

Preliminary research showed transformers exceeding temperature limits when loaded to approximately 130%. Therefore, the overload cases range from 100% to 130% loading with increments of 10%. These overload cases serve the purpose of showing the effects of transformer overloading and give insight in the consideration between using congestion management and accepting additional depreciation, as described in section 3.4.

Each case contains a time series of the ambient temperature $\theta_a(^\circ C)$ and load $S(MVA)$ per transformer. Additionally, the bus voltage of the transformer's low-voltage side is also included if available. Changes in voltage affect the current flowing through a transformer. This current affects the load factor K, as defined in equation 3.1, and thereby the loading of the transformer. An example of the input data per case is given in table 3.2. As can be seen, the time-interval is 15 minutes which is the smallest time interval available.

Timestamp	$S(MVA)$	$\theta_a(^\circ C)$	$\theta_o^{measured}(^\circ C)$	$\theta_h^{measured}(^\circ C)$	$U_2(kV)$
01-01-2022 12:00:00 AM	12.06	12.6	20.57	23.44	10.45
01-01-2022 12:15:00 AM	11.67	12.6	20.56	23.37	10.42
01-01-2022 12:30:00 AM	10.90	12.6	20.47	23.27	10.41
01-01-2022 12:45:00 AM	12.32	12.6	20.47	23.44	10.47
01-01-2022 13:00:00 AM	11.40	12.5	20.47	23.40	10.52

Table 3.2: Case data of a single transformer where S is the load, θ_a is the ambient temperature, $\theta_o^{measured}$ is the measured top-oil temperature, $\theta_h^{measured}$ is the measured hot-spot temperature and U_2 is the measured operating voltage on the transformer's low side.

The transformer's load, top-oil and hot-spot temperature are measurements at the substation. The ambient temperature time series are hourly measurements at the nearest weather station of the Royal Netherlands Meteorological Institute [18, 19].

4

Cases & results

An overview of the substations selected to construct the cases is presented in table 4.1. The cases presented here are selected from substations where the needed data, as presented in table 3.2, was available. Due to differences in demand and generation profiles, at least one substation per respective profile is selected. Stations were selected based on the availability and quality of data , for which the conditions are stated in section 3.5.

Substation	Profile	Congestion	Transformer	Type	HV-side (kV)	LV-side (kV)
1	Demand	No	1: 77 MVA	ONAN	150	10
2	Demand	Yes	1: 63 MVA	ONAF	150	10
3	Generation	Yes	121: 101 MVA	ONAF	150	20
4	Generation	Yes	121: 100 MVA	ONAF	150	20

Table 4.1: Substations which are selected to construct the cases.

The load profiles of substations 1 and 2 primarily consist of electrical demand. Substation 1 has a flat profile due to a relatively large customer with constant demand. However, it is not in congestion and its transformers are loaded to about a third of their rating. Substation 2 is in congestion and its transformers are loaded to around 80% of their rating. Furthermore, substation 2 has a more dynamic demand profile compared to substation 1.

Substations 3 and 4 have load profiles primarily consisting of electrical generation. These generation profiles are caused by an abundance of solar generation in the area where both these substations are situated. Both these substation are in congestion, though the congestion is caused due to limitations in the HV system, which is the responsibility of the TSO.

4.1. Base cases

In this section, the load profile and resulting thermal loading are presented per substation. The load profiles show the actual loading of each transformer in 2022. The thermal loading is shown by plotting the simulated and measured temperatures resulting from a load factor K in a scatter plot. By presenting the thermal loading in this way, simulated and measured temperatures can be compared easily and differences between the two can be identified.

The base cases which are modeled using standard parameters are presented in appendix A. The model with standard parameters had a MAPE between 8% and 72%, which needed to be reduced. The thermal loading results presented in this section are simulated using manually fitted transformer models, which were manually fitted as described in section 4.2.

4.1.1. Substation 1

The load profile and static limit of substation 1's transformer are shown in figure 4.1. At some time intervals the transformer does not transfer electricity. On these occasions the load is switched to the

other transformer of the substation as shown in figure A.1 in appendix A. The load profile in figure 4.1 has relatively constant demand profile and the load is highest in January and December of 2022. Additionally, the profile seems to have a cyclic behaviour. It is apparent in this case that the transformer is loaded under its limit by a significant amount as the load factor is around $K = 0.47$ at maximum.

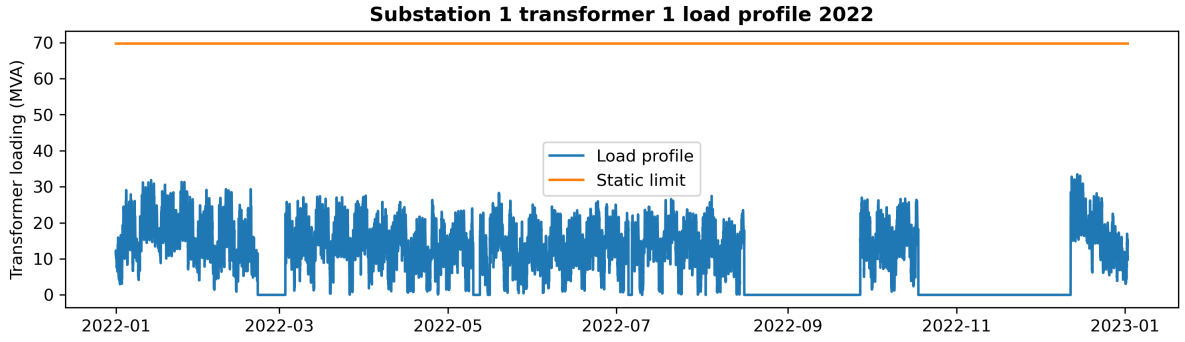

Figure 4.1: Load profile of substation 1 in 2022.

The thermal loading is presented in figure 4.2. Interestingly, both the hottest top-oil and hot-spot temperatures do not occur at the highest load factor but around $K = 0.3$.

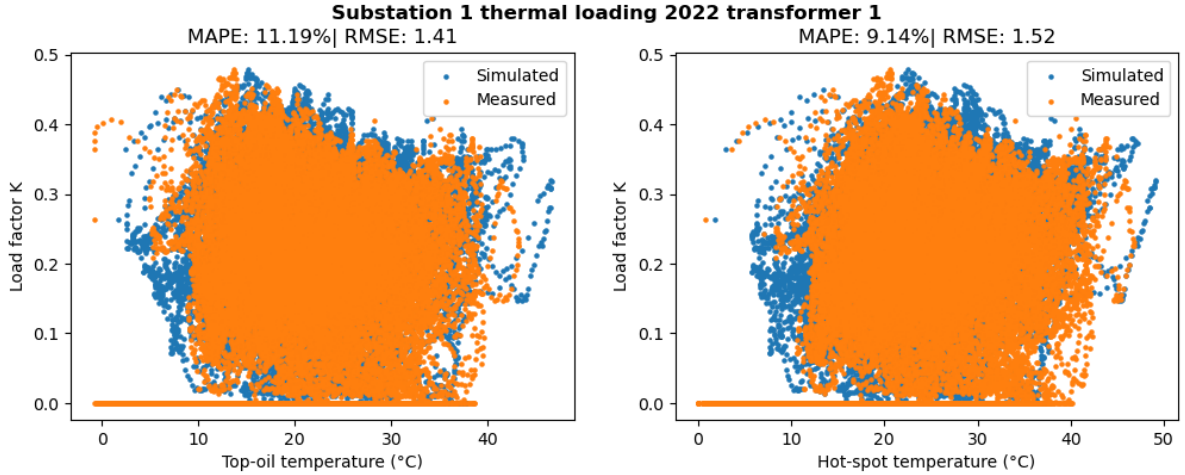

Figure 4.2: The thermal loading resulting from the load profile presented in figure 4.1.

4.1.2. Substation 2

The load profile of substation 2 is shown in figure 4.3 and contains moment without load. From figure A.3 in appendix A can be determined this is due to switching load between the substation's transformers. The load profile for this case is loaded highest in winter, reaching a load factor of around $K = 0.85$ and has a cyclic behaviour.

The thermal loading of substation 2 is shown in figure 4.4. Compared to the measured top-oil temperature scatter, the simulated top-oil temperature has a similar scatter shape. Yet, between load factor $K = 0.4$ and $K = 0.7$ there is a spike in the simulated top-oil temperatures.

The measured hot-spot temperatures of this base case tend to have its highest hot-spot temperatures at highest load factor. The simulated hot-spot temperatures show similar behaviour, however with significant deviation in the highest hot-spot temperatures.

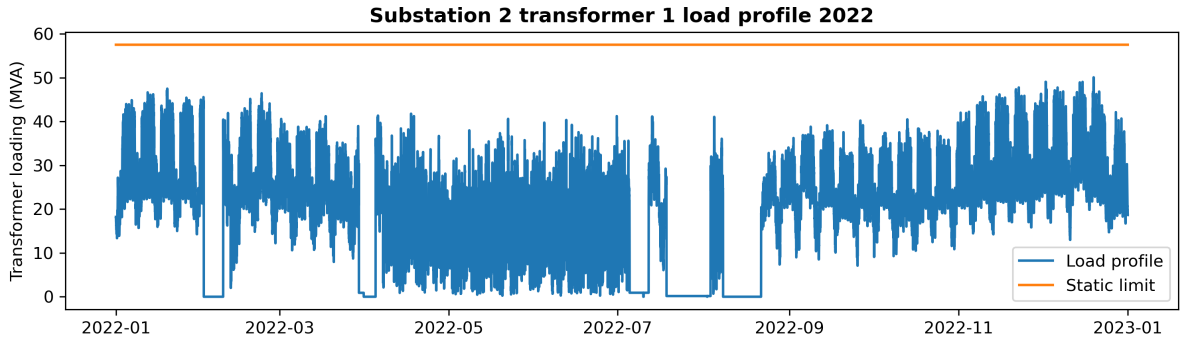

Figure 4.3: Load profile of substation 2 in 2022.

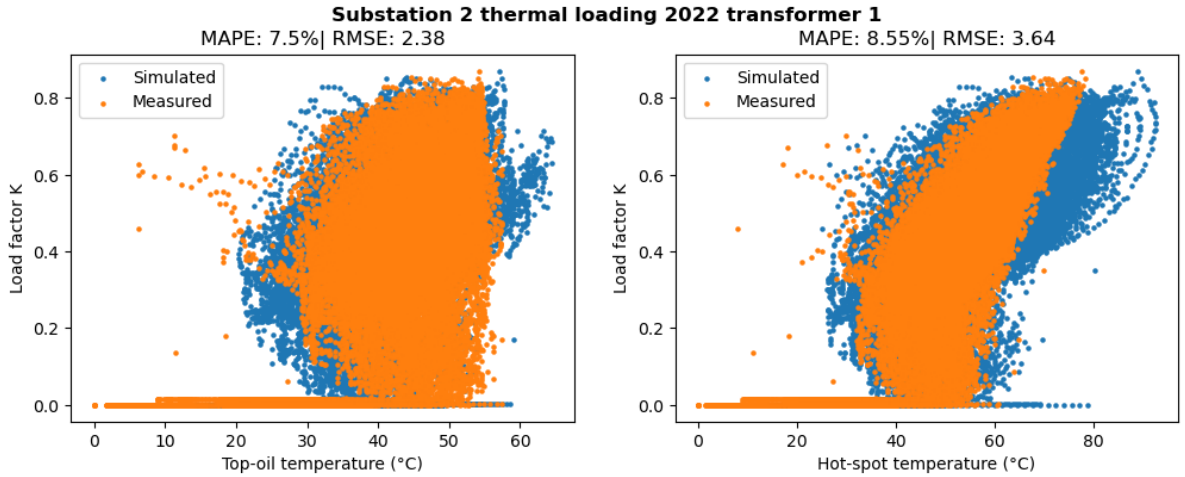

Figure 4.4: The thermal loading resulting from the load profile presented in figure 4.3.

4.1.3. Substation 3

The load profile of substation 3 is presented in figure 4.5. This load profile is more dynamic than the demand cases and loads the transformer to around $K = 0.75$ at maximum. Furthermore, this profile does not seem to have any cyclic behaviour.

The thermal loading of substation 3 is shown in figure 4.6. The simulated top-oil and hot-spot temperatures seem to have a significant overlap with their measured values. The error metrics of this case are higher compared to both demand cases.

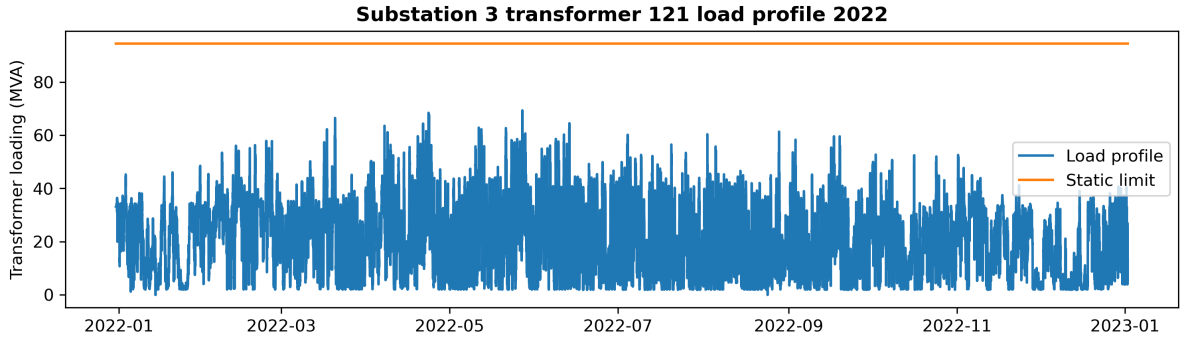

Figure 4.5: Load profile of substation 3 in 2022.

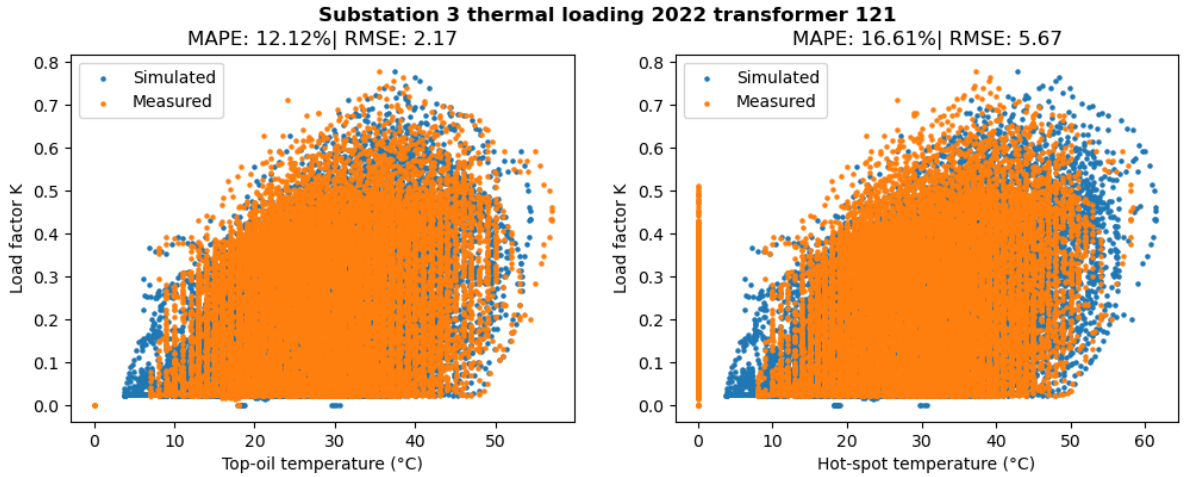

Figure 4.6: The thermal loading resulting from the load profile presented in figure 4.5.

4.1.4. Substation 4

Substation 4's base case profile is presented in figure 4.7. The transformer is more dynamic dynamically loaded compared to substation 3. Furthermore, in the thermal loading presented in figure 4.8 it is apparent that the simulated hot-spot temperatures have a significant difference compared to its measured values.

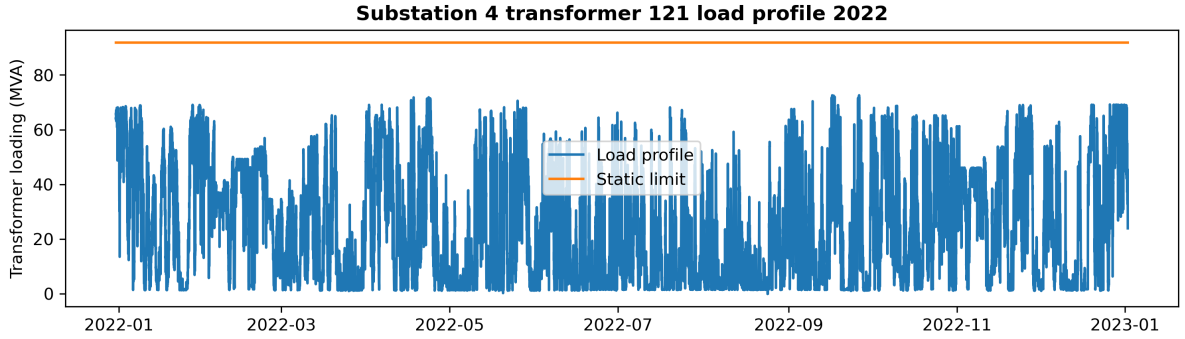

Figure 4.7: Load profile of substation 1 in 2022.

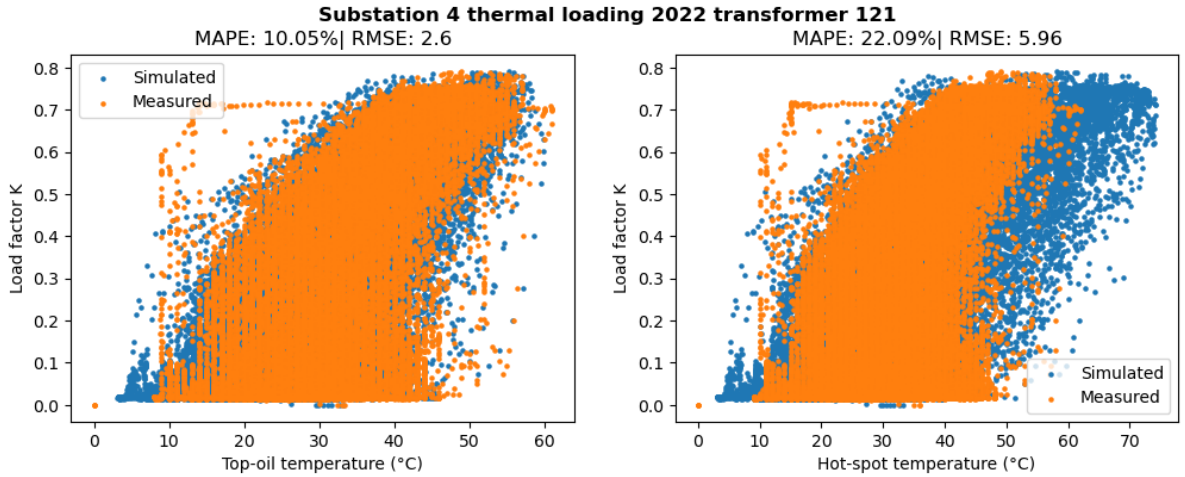

Figure 4.8: The thermal loading resulting from the load profile presented in figure 4.7.

4.2. Curve fitting results

The thermal loading results presented in section 4.1 are simulated using curve fitted models. However, these curve fitted models are created using the curve fitting method presented in section 3.3 and are based on models using standard parameters. This section presents the changes in error metrics of the transformer temperature models used for each transformer.

The curve fitting method resulted in an overall reduction of error metrics, as shown in table 4.2. The models using curve fitted parameters showed a decrease in RMSE and MAPE, compared to the model using standard parameters. This decrease is observed for both the top-oil and hot-spot temperature, with one exception in the top-oil temperature RMSE and MAPE of station 3. The decrease in hot-spot temperature RSME and MAPE is more significant, compared to the decrease in RMSE and MAPE of the top-oil temperature. Where the decrease in MAPE of the top-oil temperature is between 1 and 5 percentage points, the decrease in hot-spot temperature MAPE is between 14 and 52 percentage points.

Although the curve fitting method reduced the RMSE and MAPE in the models, the simulated top-oil and hot-spot temperature showed different behaviour over time when compared to the measured values. This behaviour is elaborated on in appendix B per substation. To correct this behaviour, the model parameters have been manually changed. This manual fitting process is explained further in appendix B.

A common characteristic in the thermal behaviour of each base case was a delayed reaction of the top-oil and hot-spot temperatures simulated by the curve fitted models. In every base case, except for substation 3, the time constants where decreased to reduce the delayed reaction.

Some models tended to undershoot the simulated hot-spot temperature. This undershoot is unwanted as the additional ageing is an exponential function of the hot-spot temperature. Undershoot of the simulated hot-spot temperature would therefore benefit depreciation costs and skew the cost comparison between congestion management and additional depreciation. The parameters in the manual fitting process were therefore chosen such that the simulated hot-spot temperatures always overshoot. This overshoot can be considered as a safety factor.

Although the manual fitting process resulted in improved thermal behaviour of simulated top-oil and hot-spot temperatures, the error metrics increased. Theoretically, this increase is a reduction in model accuracy. However, due to the improved thermal behaviour shown in appendix B and overshoot described in the previous paragraph, the manually fitted parameters are used in modeling the base and overload cases.

Station	**Standard parameters**				**Curve fitted parameters**				**Manually fitted parameters**			
	Top-oil temperature		*Hot-spot temperature*		*Top-oil temperature*		*Hot-spot temperature*		*Top-oil temperature*		*Hot-spot temperature*	
	RMSE	MAPE	RMSE	MAPE	RMSE	MAPE	RMSE	MAPE	RMSE	MAPE	RMSE	MAPE
1	1.6	12.95	6.54	43.78	1.01	7.4	1.29	7.36	1.41	11.19	1.52	9.14
2	4.13	13.85	8.82	23.68	2.38	7.5	3.95	9.5	2.38	7.5	3.64	8.55
3	1.72	8.49	11.05	52.2	1.8	9.26	4.29	10.56	2.17	12.12	5.67	16.61
4	2.71	11.28	16.55	72.42	2.63	10.15	5.48	20.34	2.6	10.05	5.95	22.09

Table 4.2: Error metrics for standard parameters, curve fitted parameters and manually fitted parameters.

4.3. Overload cases

Overload profiles of substations 1 and 2 are presented in figures 4.9 and 4.11. What is apparent at first is the volume of the load exceeding the limit in both substations.

The simulated temperatures are presented in figures 4.10 and 4.12. As can be seen, the hot-spot temperature limits are increasingly exceeded in the 110%, 120% and 130% profiles.

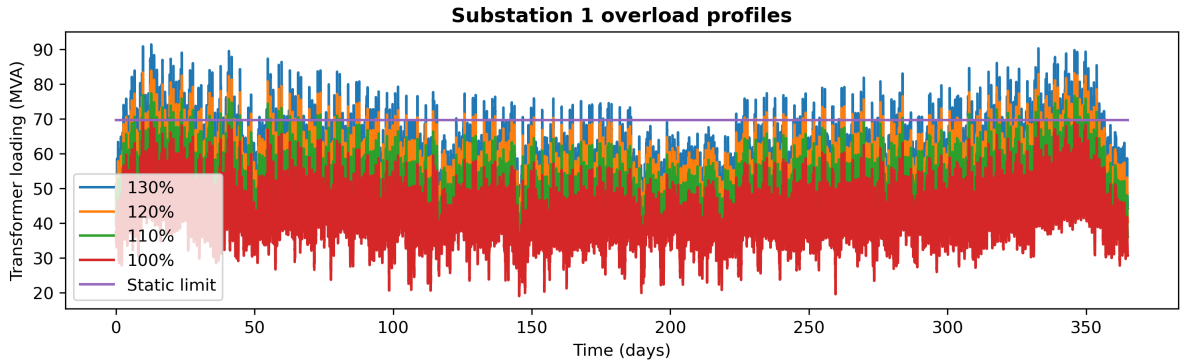

Figure 4.9: Load profiles of overload cases substation 1

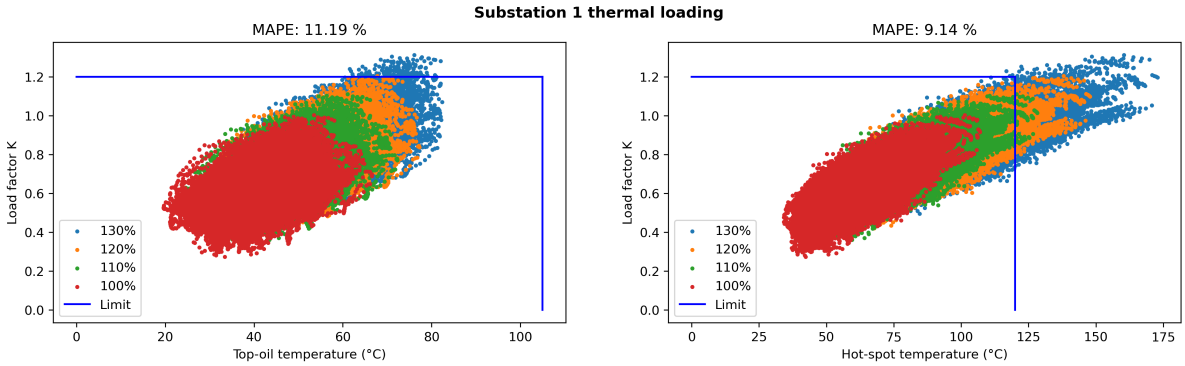

Figure 4.10: Simulated temperatures due to overloading of transformer 1 in substation 1

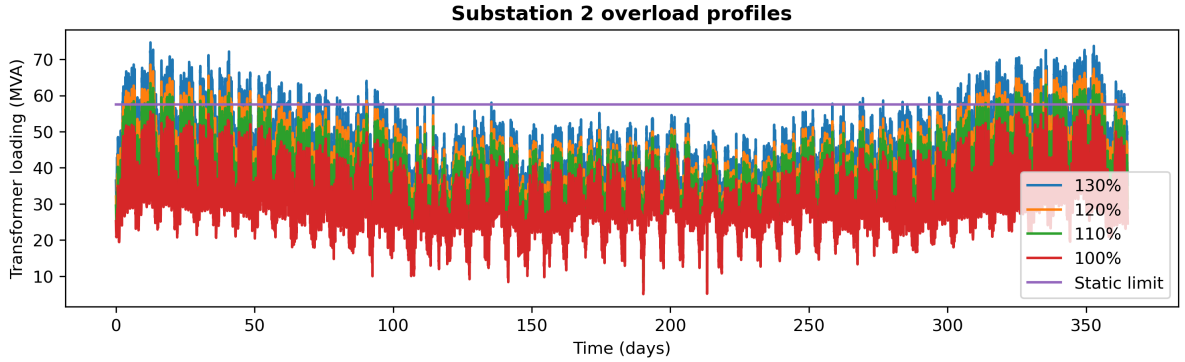

Figure 4.11: Load profiles of overload cases substation 2

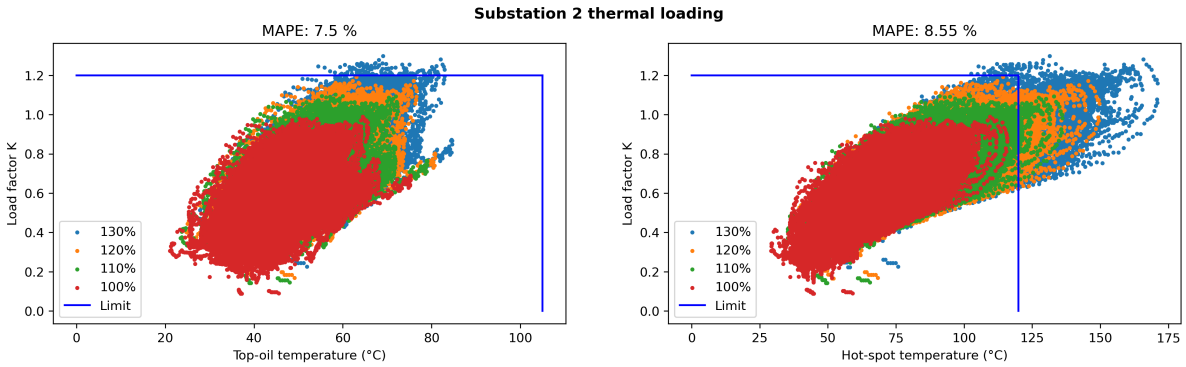

Figure 4.12: Simulated temperatures due to overloading of transformer 1 in substation 2

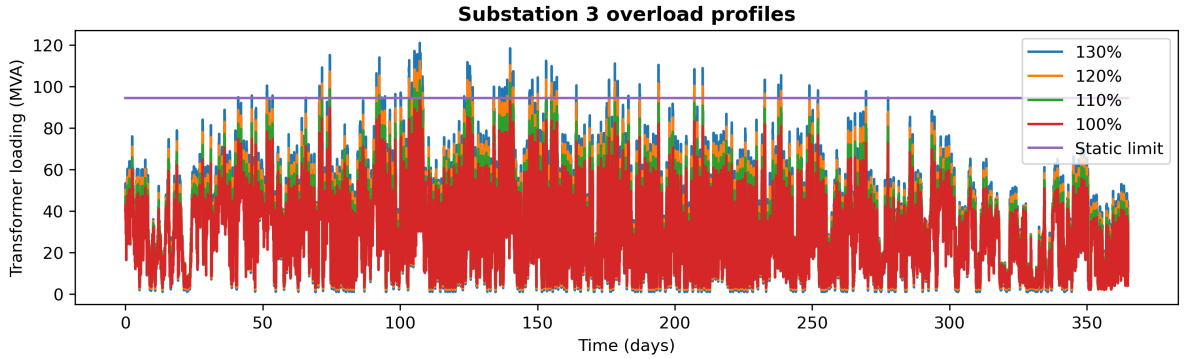

Figure 4.13: Load profiles of overload cases substation 3

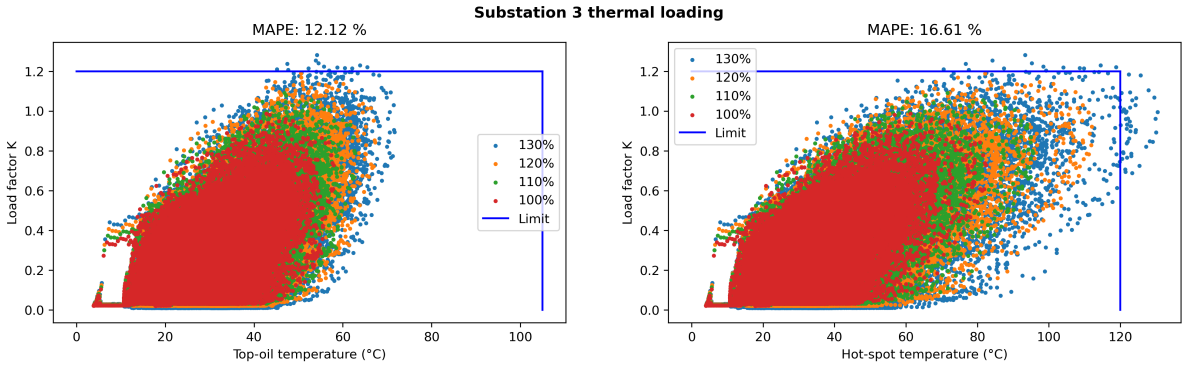

Figure 4.14: Simulated temperatures due to overloading of transformer 1 in substation 3

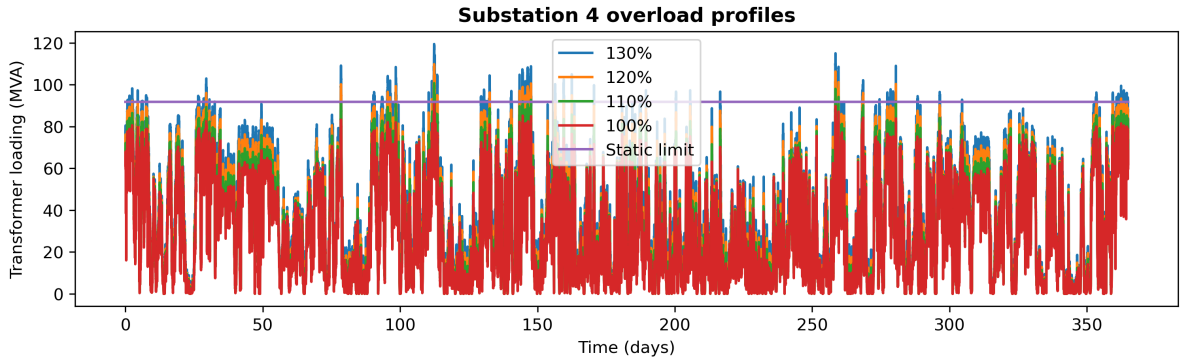

Figure 4.15: Load profiles of overload cases substation 4

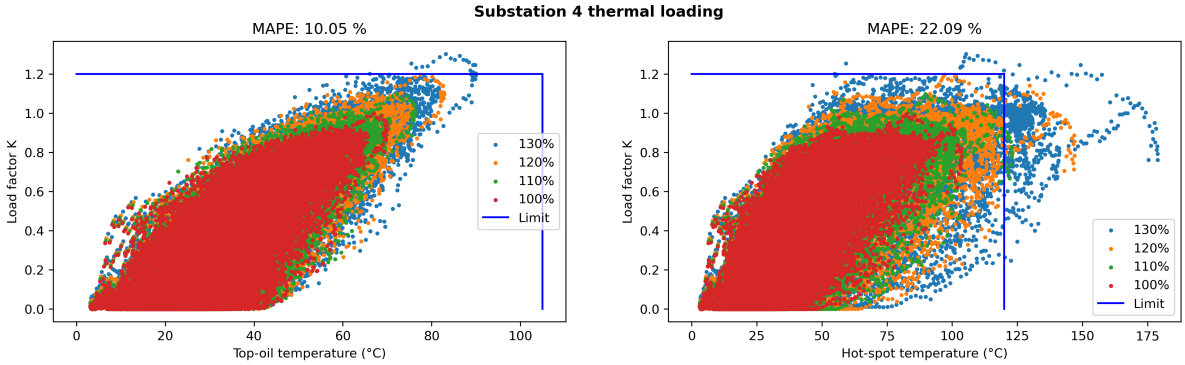

Figure 4.16: Simulated temperatures due to overloading of transformer 1 in substation 4

When comparing the demand profile cases with generation profile cases, it is apparent there is a significant difference in thermal loading. Where the overload cases with demand profiles exceed temperature limits at 110% loading, the cases with generation profile exceed these limits at 130% loading. Furthermore, the difference in amount of energy by which the transformer is overloaded is apparent when comparing demand and generation profiles. The energy volume above the limit is larger in figures 4.13 and 4.15, when compared to figures 4.9 and 4.11.

The difference in profile is also apparent in comparing costs of additional depreciation and congestion management. Figure 4.17 presents the costs of additional depreciation and congestion management per overload case per station. The congestion management costs in cases with demand profile are significantly higher compared to those with a generation profile. Furthermore, the costs of additional depreciation are higher in both cases with demand profile.

Additionally, the figure shows both costs increase with overloading percentage. However, congestion management costs seem to ramp up faster compared to additional appreciation, at least to overloading of 130%. Though a significant difference is observed between substation 3 and 4, as additional depreciation costs of substation 3 remained low, the additional depreciation costs of substation 4 increase significantly at 130% overloading.

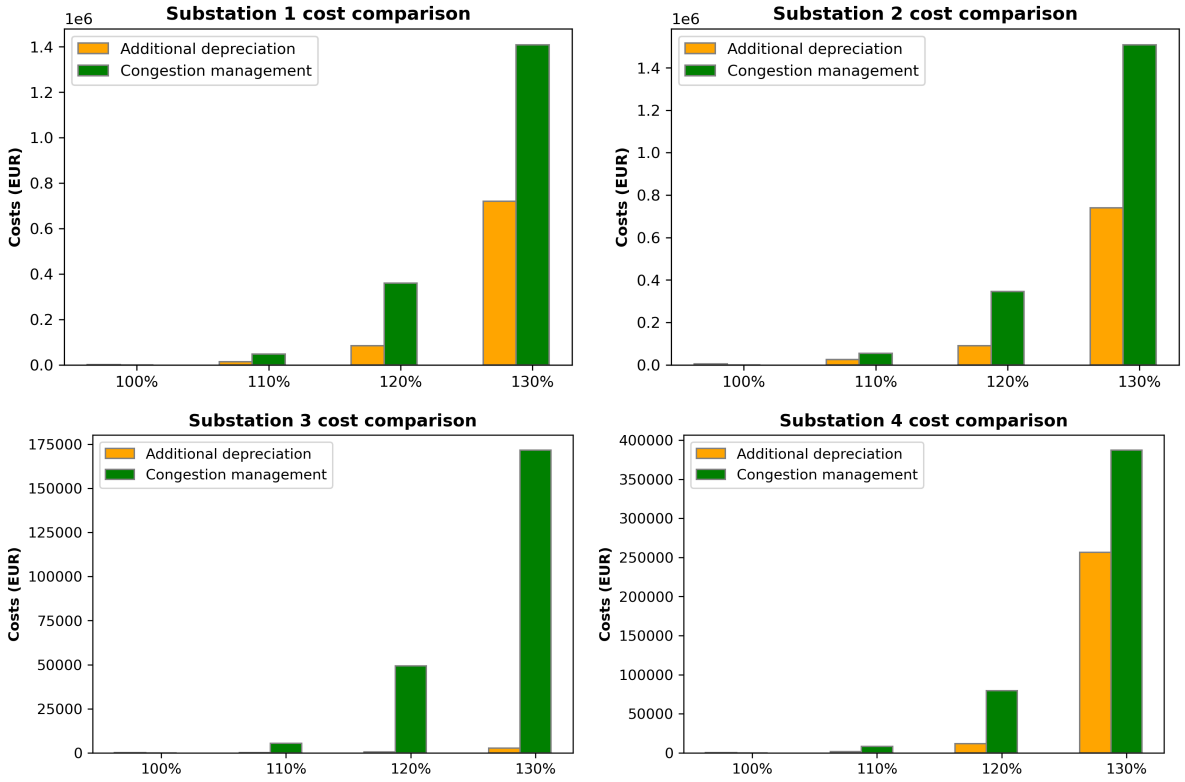

Figure 4.17: Cost comparison between additional depreciation due to overloading and congestion management

5

Discussion & recommendations

5.1. Discussion

The loading guide model using standard parameters showed inaccuracy in simulating top-oil and hot-spot temperatures, with inaccuracy of the hot-spot temperatures being more significant. The curve-fitting method showed an increase in accuracy but also disconnected thermal behaviour between observed and simulated values. As a result, parameters had to be manually fitted to match thermal behaviour of simulated and measured values. The model using manually fitted parameters has an inaccuracy between 7.5% and 22%. This inaccuracy can be attributed to the manual fitting of model parameters aiming for overshoot, so simulated values would be larger than measured. This overshoot is considered a safety factor.

Additionally, in this research a key point is including observed ambient temperature in modeling the dynamic rating of transformers. However, dynamic rating of transformers is not solely based on ambient temperature. Other influences such as irradiation, wind and rain affect dynamic rating of transformers. These influences were not considered in this research and are a possible source of the inaccuracy and observed differences.

Lastly, research relies heavily on measured data which was assumed to be true and of perfect quality. This assumption is another source of inaccuracy.

Significant differences in thermal loading during overload scenarios were observed between cases with demand and generation profiles. Cases with demand profiles reached significantly higher hot-spot temperatures compared to cases with generation profiles. This difference can be attributed to the characteristics of demand and generation profiles. Generation profiles are generally low base load with high peaks, while demand profiles have a high base load with small peaks. Due to this difference, when a demand profile is used in overloading, the volume of the energy near or above the limit is greater compared to generation profiles. This difference between demand and generation profiles causes demand profiles to cause more severe thermal loading on a transformer.

The difference between additional depreciation and congestion management costs is significant. However, the additional depreciation costs are dependant on an exponential function with simulated hot-spot temperature as input. This input has an inaccuracy which can affect the additional depreciation costs and can change the outcome of the cost comparison. Furthermore, re-dispatch costs are also subject to change as the price used is heavily influenced by the recent energy crisis in the Netherlands. The expectation is these costs, and thereby congestion management costs, will decrease. Both these effects could change both costs significantly and change the outcome of the cost comparison.

5.2. Further research

The costs of additional depreciation are based on linear depreciation in this research. However the costs of overloading can also be expressed as loss of net present value (NPV), which is a more realistic scenario. Using this NPV can change the difference between additional depreciation and congestion

management costs and should be considered in further research.

The model showed inaccuracies after curve fitting. These inaccuracies could stem from the quality of the input data. In this research the input data is assumed to be correct, which is not true in practice. Further research in the form of a stochastic analysis could provide insights into the quality of the input data used in this research and could improve the accuracy of the loading guide model.

Further research in application of the loading guide for modelling dynamic rating should strive for applications in specific time-frames. In this research, the time-frame for all cases was a year, which was computationally intensive and time-consuming. However, the important events in terms of overloading tend to happen multiple times each year and with the same characteristics. It would therefore be more time-efficient to identify these specific events and model accordingly.

5.3. Takeaways for Enexis

The method presented here could be suitable for implementation in Enexis' operations. The cases used in this research are based on empirical data, however, the model supports use of forecast data. For instance, forecasts of substation load and ambient temperature can be combined to generate forecasts of transformer loading. This forecast presents the opportunity for operations to see whether a transformer is going to exceed its limits intra-day or day-ahead. However the additional error of using forecasts as input data should be considered.

When revisiting policy for loading HV/MV transformer above nominal rating, Enexis should consider using a more accurate model than the loading guide. The loading guide is a fairly simplified model which uses parameters determined emperically. In this research, MAPE of between 8% and 72% were observed between measured and simulated values when using the loading guide with standard parameters. This inaccuracy could be reduced to between 7% and 22% using curve fitting. However, this inaccuracy can still mean the difference between touching on the limits of a transformer's loading and wiping of its entire lifetime during one overload scenario. Therefore, Enexis should consider using a more accurate model for determining transformer overloading policy.

6

Conclusions

Primary components have dynamic rating due to their thermal capacity and when being subjected to dynamic conditions. This thermal capacity is related to mass, which is why low mass components' dynamic rating has less potential. It was determined HV/MV transformers have high potential for dynamic rating due to their high mass.

The ability of HV/MV transformers to provide additional capacity depends on the configuration of the substation and whether the transformer is the limiting component. It can therefore be concluded that if the transformer is a station's limiting component and its dynamic rating is taken into account, transformers can provide additional capacity through loading above their nominal rating.

The dynamic rating of HV/MV transformers can be modeled using differential equations based on thermodynamics. The modeling results showed transformers can be overloaded when using dynamic rating. The amount of overloading which can be accepted differed between demand and generation profiles. Cases with demand profiles showed simulated temperatures exceeding the limits when the transformers where loaded to a maximum of 110%. In contrast, cases with generation profiles the transformers were able to accept a maximum of 120% loading before temperature limits were exceeded.

Dynamic rating in congestion management scenarios showed a cost comparison. This effect is a consideration between the additional ageing due to overloading and costs for congestion management. The costs of additional depreciation due to ageing showed to be significantly lower compared to costs of using congestion management budget to re-dispatch or curtail the excess energy. However it should be noted that additional depreciation is simulated using a model dependant on transformer specific parameters which can introduce significant inaccuracy.

References

[1] Netbeheer Nederland. *Het energiesysteem van de toekomst: de II3050-scenario's*. Tech. rep. 2023.

[2] TenneT. *TenneT's netcapaciteitskaart*. 2023. URL: https://www.tennet.eu/nl/de-elektriciteitsmarkt/congestiemanagement/netcapaciteitskaart.

[3] Netbeheer Nederland. *Capaciteitskaart elektriciteitsnet*. Dec. 2023. URL: https://capaciteitskaart.netbeheernederland.nl/.

[4] Netbeheer Nederland and Autoriteit Consument & Markt. *Landelijk Actieprogramma Netcongestie*. Tech. rep. 2022.

[5] Autoriteit Consument & Markt. *ACM onderzoekt met netbeheerders mogelijkheden om gevolgen personeelstekort te verkleinen*. Mar. 2022. URL: https://www.acm.nl/nl/publicaties/acm-onderzoekt-met-netbeheerders-mogelijkheden-om-gevolgen-personeelstekort-te-verkleinen.

[6] Alliander. *Cable pooling*. URL: https://www.alliander.com/nl/cable-pooling/.

[7] Enexis. *Efficiënter benutten van het net*. URL: https://jaarverslag.enexisgroep.nl/jaarverslag-2022/efficienter-benutten-van-het-net.

[8] Enexis. *Congestiemanagment onderzoeken*. URL: https://www.enexis.nl/zakelijk/aansluitingen/congestie-onderzoeken.

[9] Stephen R. Turns. *Thermodynamics: concepts and applications*. 1st ed. 2006. ISBN: 978-0-521-85042-1.

[10] Electrical-Technology. *12 Different Parts of Transformer and their Functions*. URL: 12%20Different%20Parts%20of%20Transformer%20and%20their%20Functions.

[11] International Electrotechnical Commision. *Power transformers-Part 7: Loading guide for mineral-oil-immersed power transformers (IEC 60076-7)*. 2018. ISBN: 9782832250822. URL: www.iec.ch.

[12] Radu Godina et al. *Effect of loads and other key factors on oil-transformer ageing: Sustainability benefits and challenges*. 2015. DOI: 10.3390/en81012147.

[13] Chris Tofallis. "A better measure of relative prediction accuracy for model selection and model estimation". In: *Journal of the Operational Research Society* 66.8 (Aug. 2015), pp. 1352–1362. ISSN: 14769360. DOI: 10.1057/jors.2014.103.

[14] Doug Peterchuck and Anil Pahwa. "Sensitivity of transformer's hottest-spot and equivalent aging to selected parameters". In: *IEEE Transactions on Power Delivery* 17.4 (Oct. 2002), pp. 996–1001. ISSN: 08858977. DOI: 10.1109/TPWRD.2002.803708.

[15] Tong Qian et al. *Multi-parametric Sensitivity Analysis of Improved Transformer Thermal Models Considering Nonlinear Effect of Oil Time Constant*. Tech. rep. 2020.

[16] Stichting GOPACS. *GOPACS: het platform om congestie in het net te verminderen*. URL: https://www.gopacs.eu/.

[17] GOPACS. *Gopacs resultaten*. URL: https://idcons.nl/#/performance-metrics.

[18] KNMI. *Automatische weerstations*. URL: https://www.knmi.nl/kennis-en-datacentrum/uitleg/automatische-weerstations.

[19] KNMI. *Uurgegevens*. URL: https://daggegevens.knmi.nl/klimatologie/uurgegevens.

A

Base case results without curve fitting

A.1. Substation 1

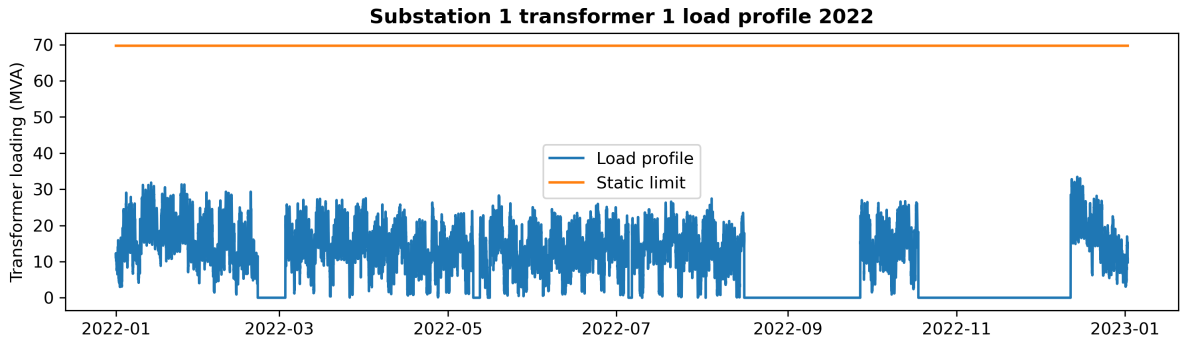

(a)

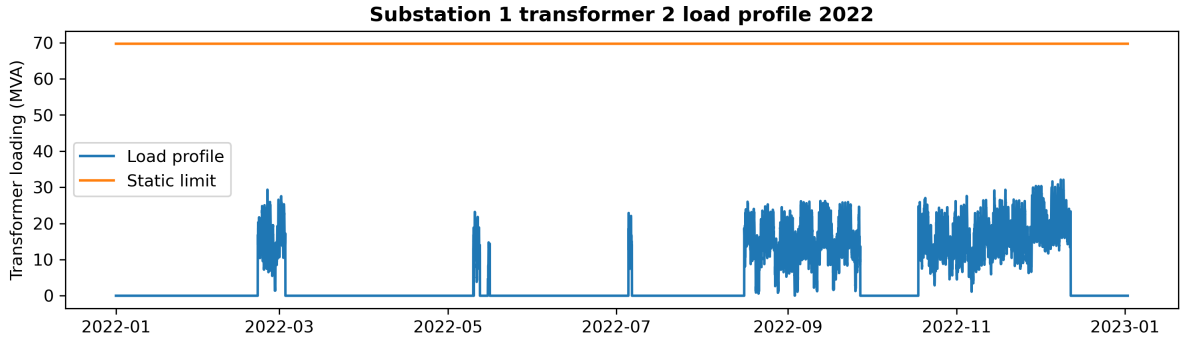

(b)

Figure A.1: Load profiles for each transformer in substation 1.

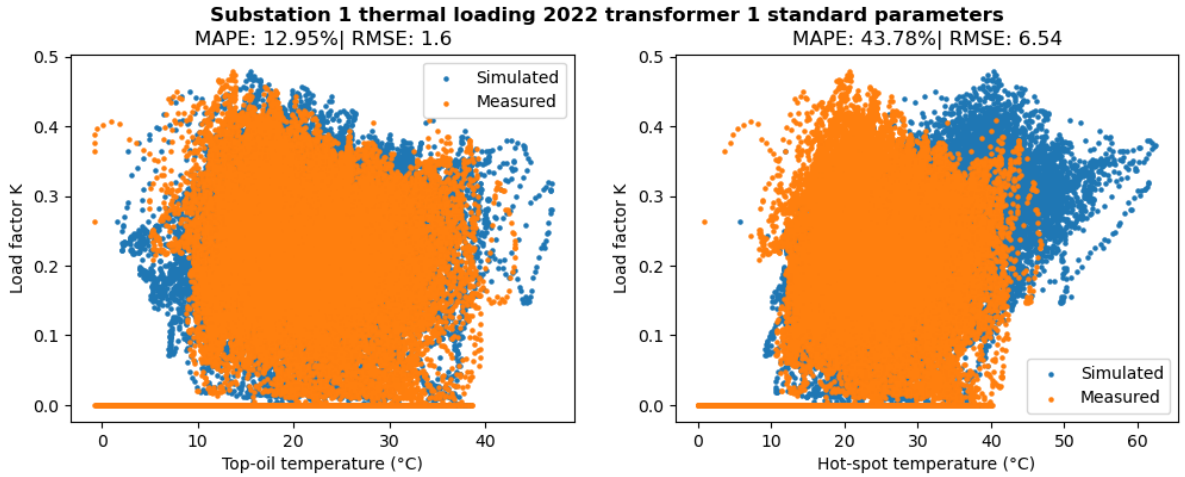

Figure A.2: The thermal loading resulting from the load profile presented in figure A.1 while using standard parameters from table 3.1.

A.2. Substation 2

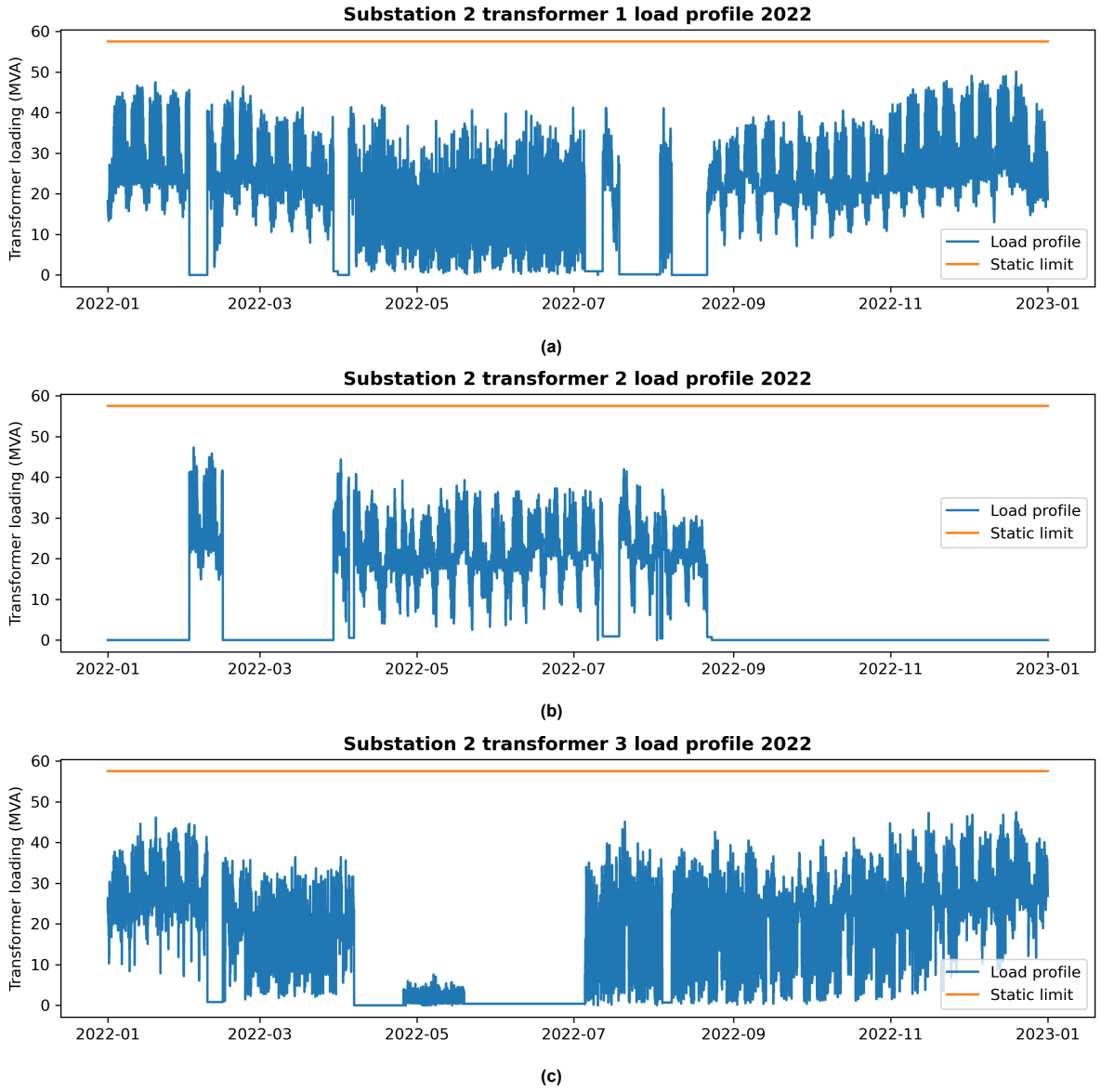

Figure A.3: Load profiles for each transformer in substation 1.

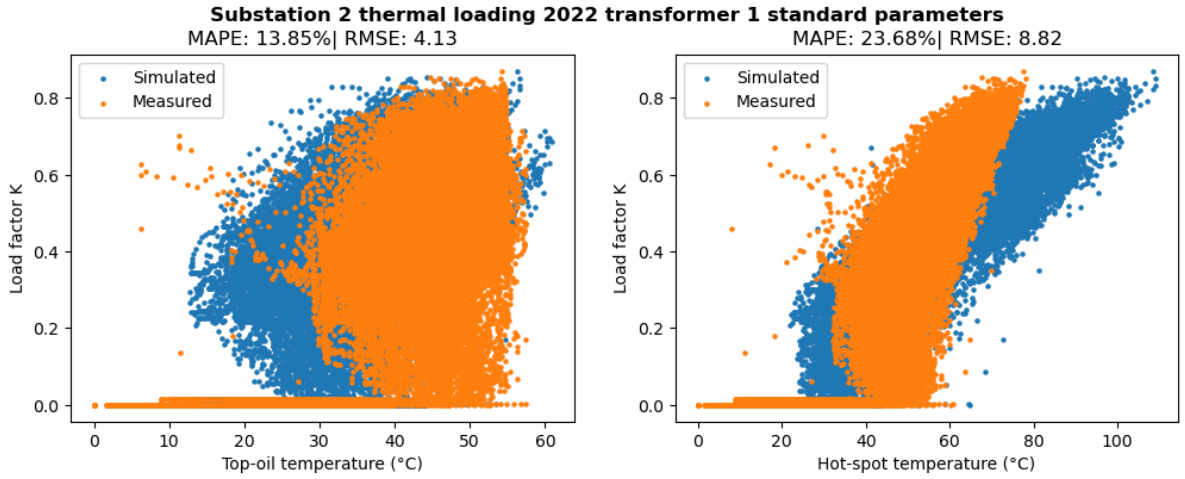

Figure A.4: The thermal loading resulting from the load profile presented in figure A.3 while using standard parameters from table 3.1.

A.3. Substation 3

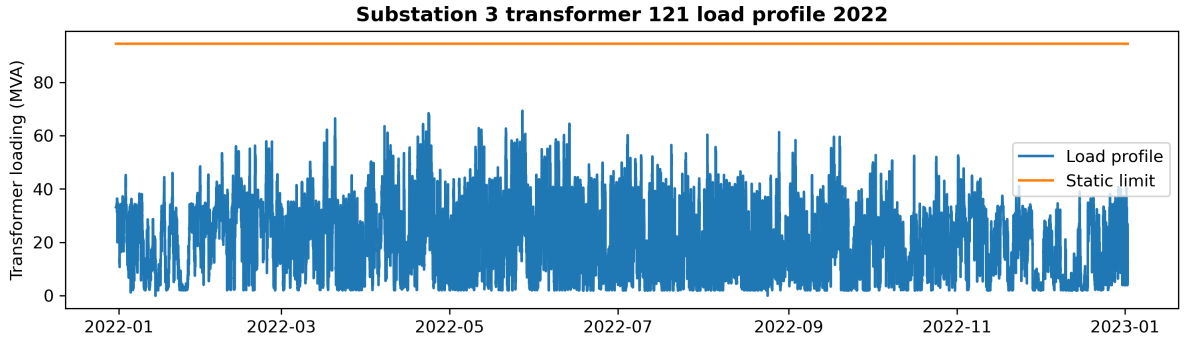

Figure A.5

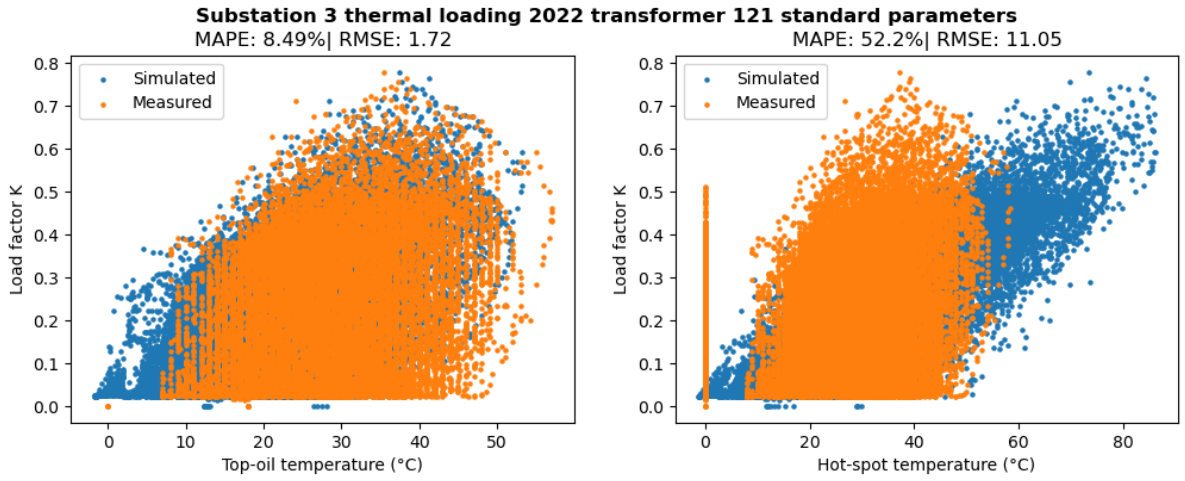

Figure A.6: The thermal loading resulting from the load profile presented in figure A.5 while using standard parameters from table 3.1.

A.4. Substation 4

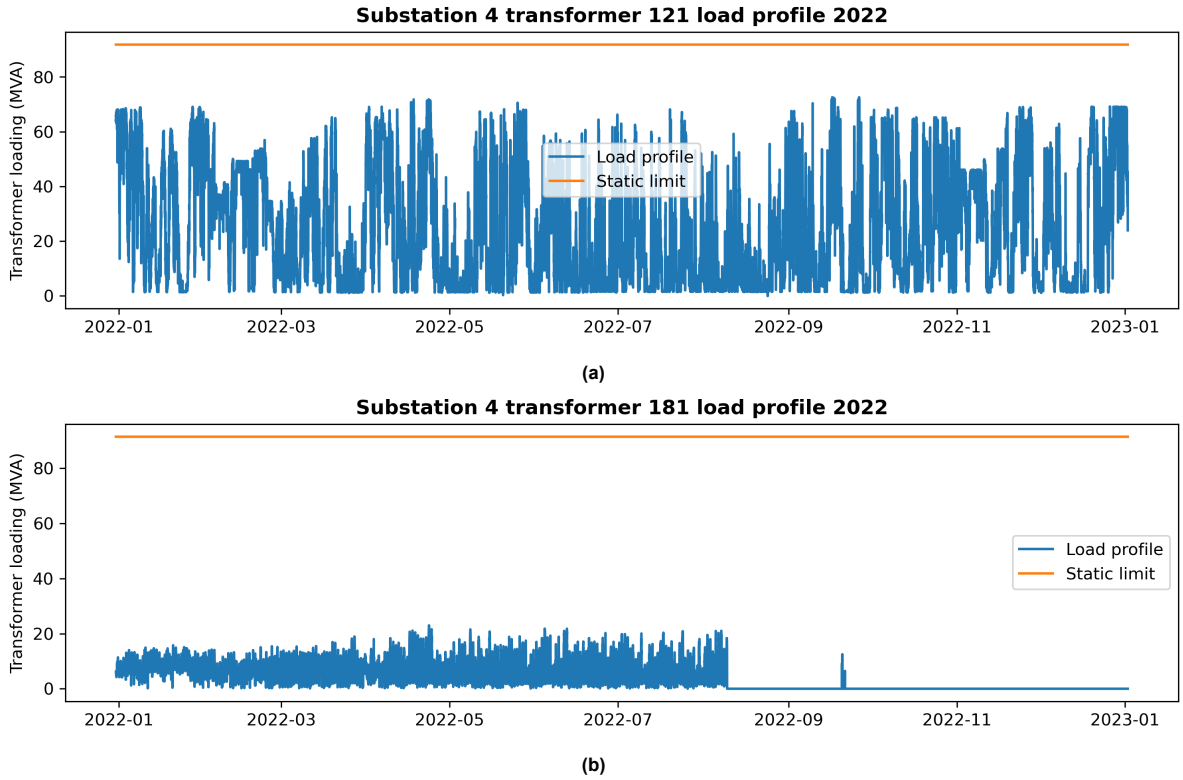

Figure A.7: Load profiles for each transformer in substation 1.

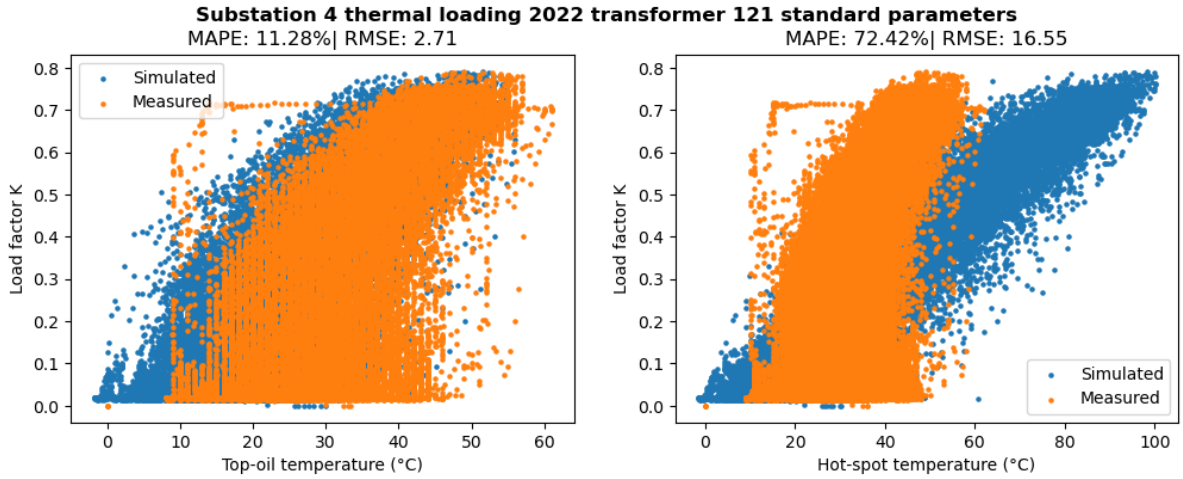

Figure A.8: The thermal loading resulting from the load profile presented in figure A.7a while using standard parameters from table 3.1.

B

Curve fitting

To investigate the thermal behaviour of the fitted model per substation, the thermal loading of a specific month is analysed. If thermal behaviour of the simulated values does not match the measured values after using the curve fitting method presented in section 3.3, manual fitting is applied. This manual fitting is achieved by changing model parameters per base case.

The general process of manual fitting uses the parameters determined by the curve fitting method as a guideline. Additionally, the curve fitting method yielded error graphs. These graphs show the set of parameters which were fitted and the resulting error metrics in a 3d-plot. Characteristics of the parameters can be identified in these graphs. The manual fitting process takes into account both the curve fitted constants and the error metric characteristics to optimize the thermal behaviour of the models.

Table B.1 presents the curve fitted and manually fitted parameters per substation. The changes of model parameters from curve fitted to manually fitted are explained for each substation in this appendix's sections.

Parameter	**Curve fitted**				**Manually fitted**			
	1	*2*	*3*	*4*	*1*	*2*	*3*	*4*
Oil exponent x	0.8	0.6	0.8	0.6	0.8	0.6	0.6	0.6
Winding exponent y	2.3	2.2	2.9	3.8	2.3	2.2	2.9	3.8
Oil time constant τ_o	700	300	300	500	300	300	500	300
Winding time constant τ_w	350	450	550	550	100	150	150	300

Table B.1: Curve fitted and manually fitted parameters

B.1. Substation 1

The thermal loading of the transformer in substation 1 during July of 2022 is shown in figure B.1. In this case, the simulated top-oil and hot-spot temperatures of the curve fitted model had a delayed reaction to changes in load factor. Therefore the time constants were reduced using the error graphs in figure B.3 and B.4. Comparing the thermal behaviour in figures B.1 and B.2, one can see the manually fitted model matches the behaviour measured temperature better. Especially the temperatures of the peaks.

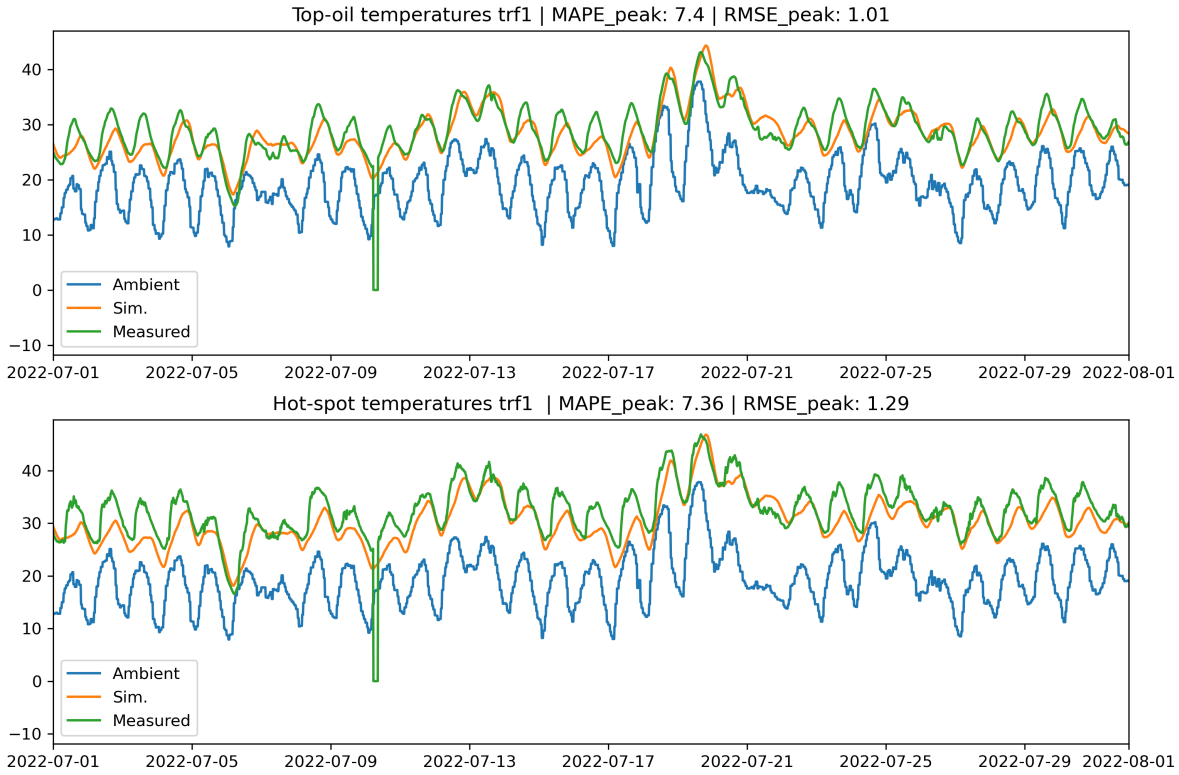

Figure B.1: Curve fitted model temperature behaviour of substation 1

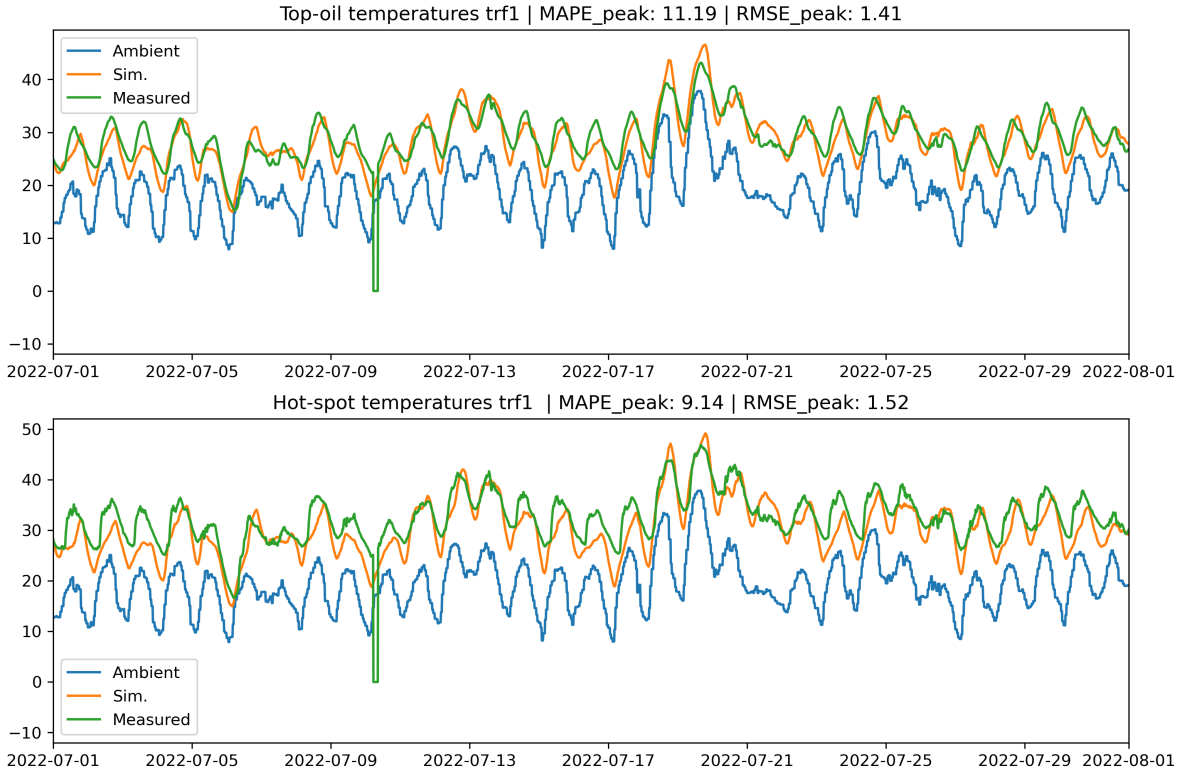

Figure B.2: Manually fitted model temperature behaviour of substation 1

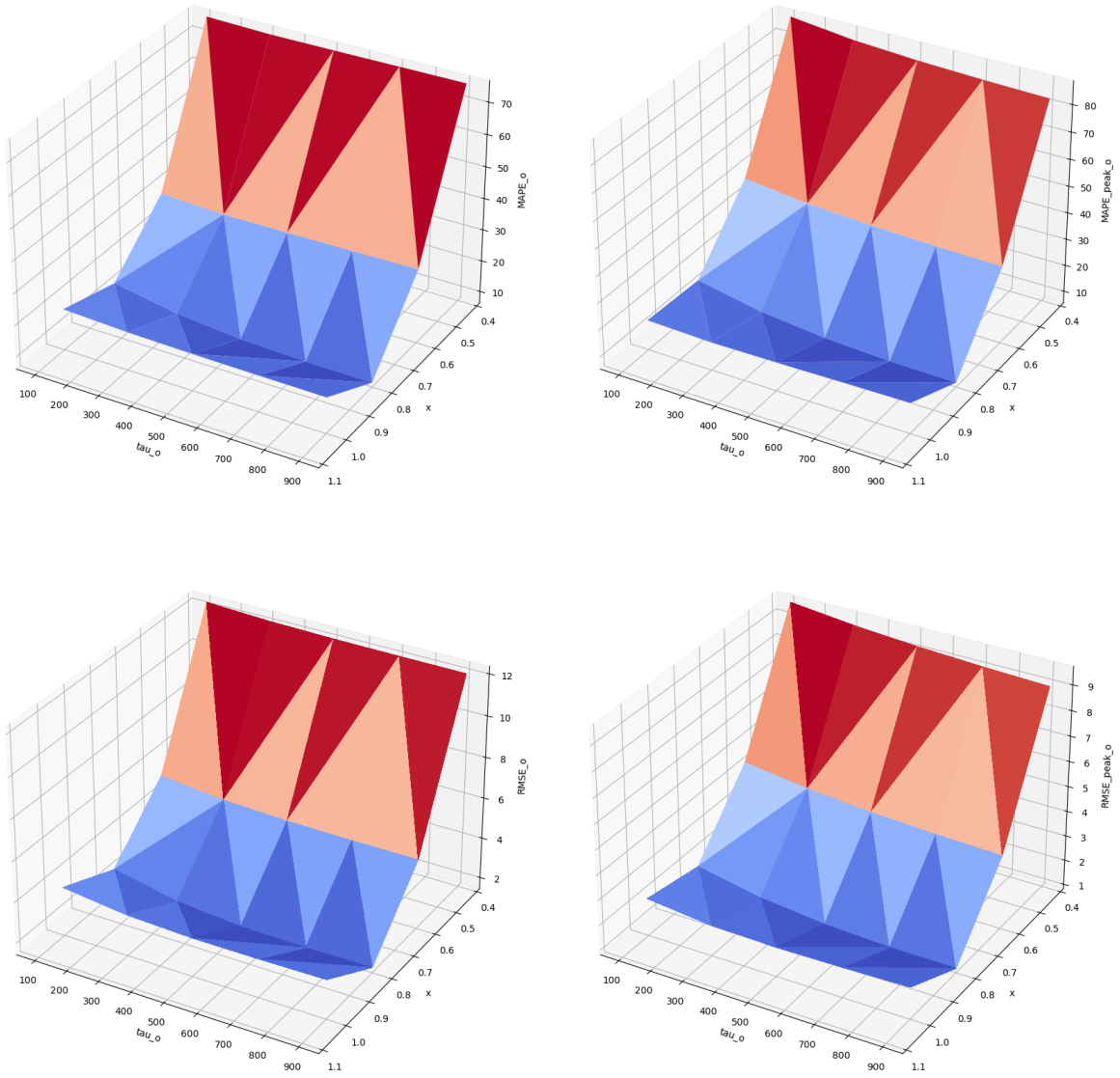

Figure B.3: Error graph for top-oil temperature of substation 1

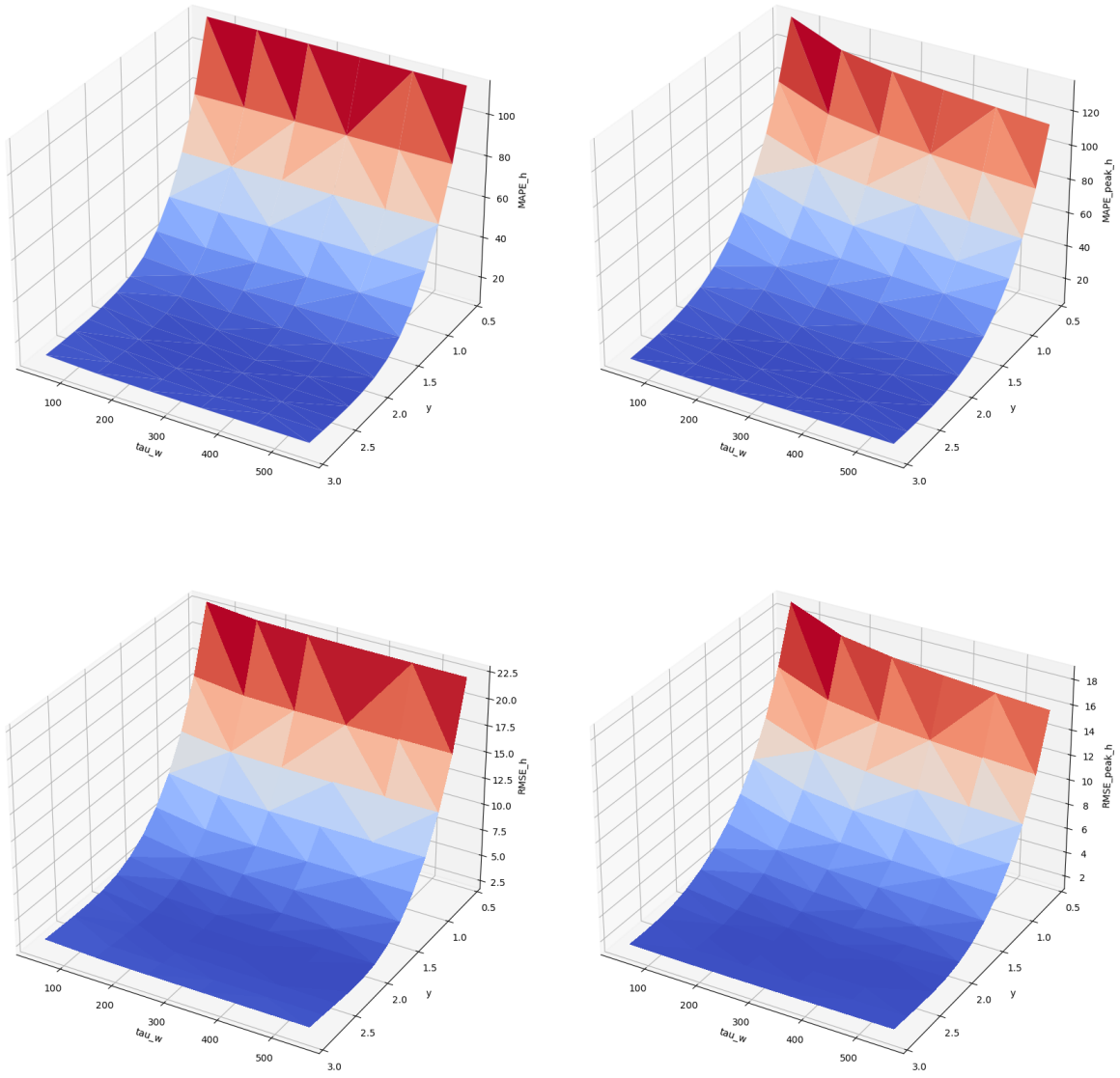

Figure B.4: Error graph for hot-spot temperature of substation 1

B.2. Substation 2

In this case, the simulated hot-spot temperature in figure B.5 shows delayed response to changes in load compared to the measured values. Therefore the winding time constant τ_w was reduced using the error graph in figure B.8 to find an optimum for the parameter. The difference of the manual parameter is clearly visible when comparing figures B.5 and B.6, as the hot-spot temperatures in the manually fitted model match the measured temperature behaviour much better.

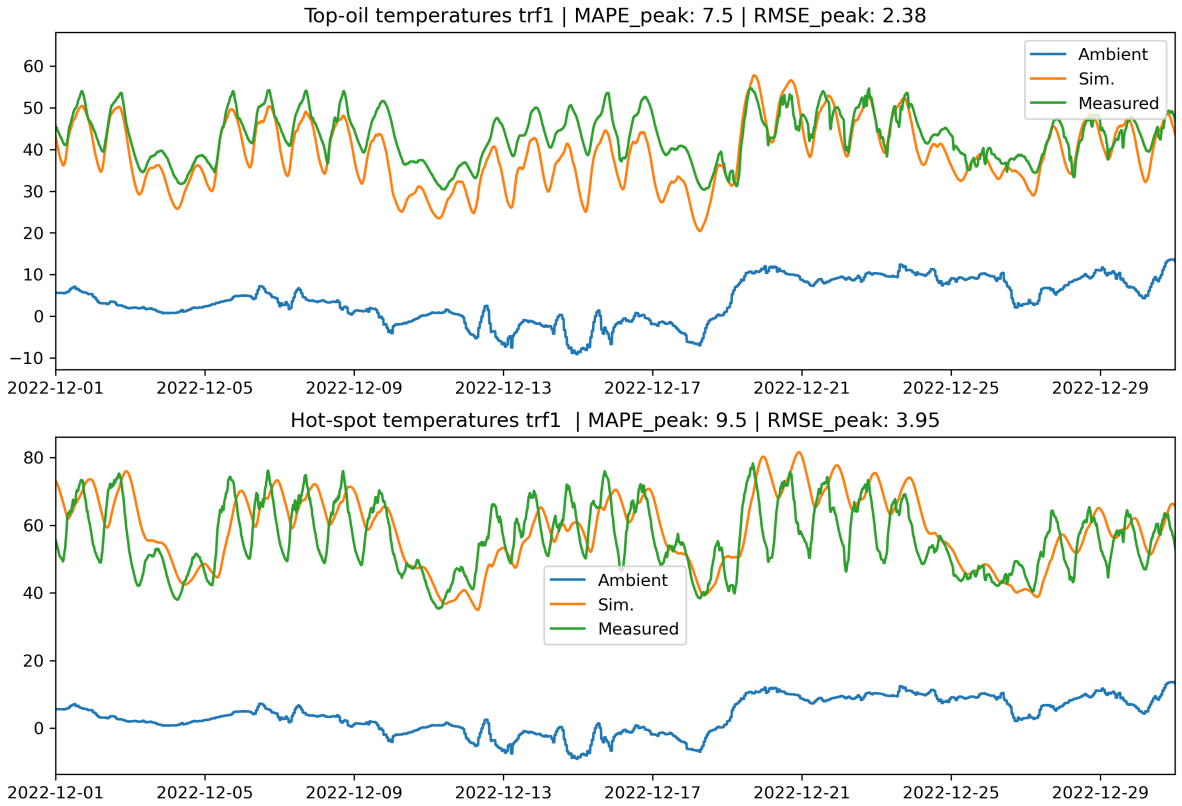

Figure B.5: Curve fitted model temperature behaviour of substation 2

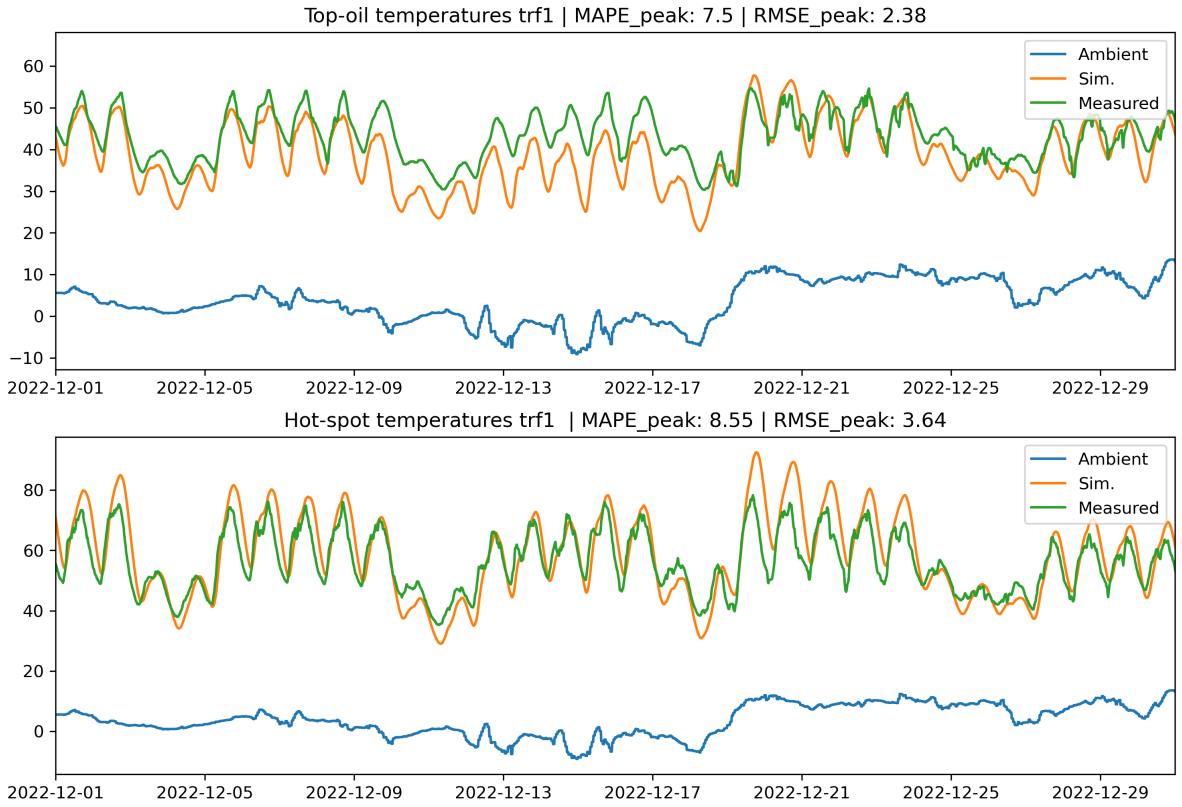

Figure B.6: Manually fitted model temperature behaviour of substation 2

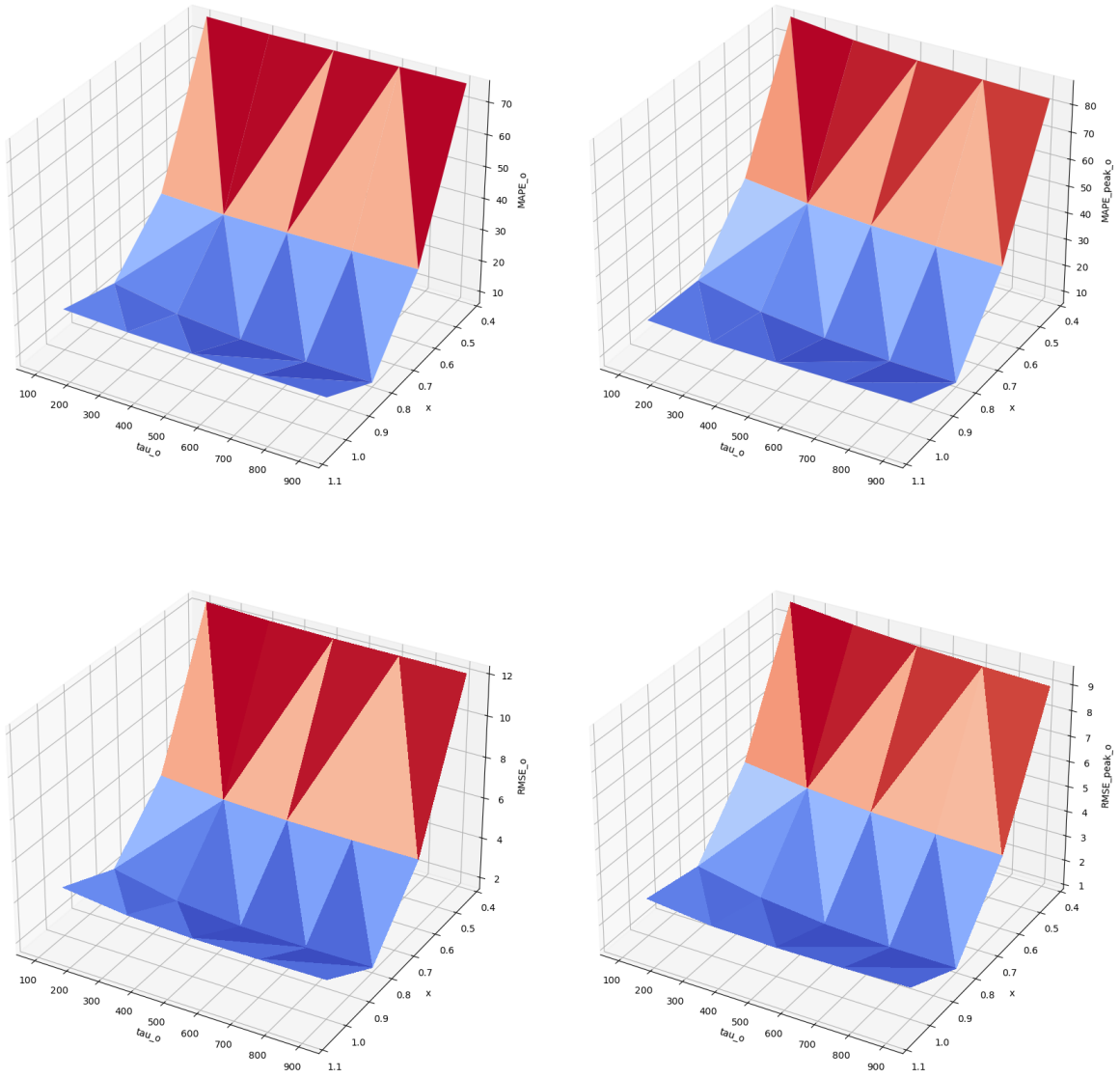

Figure B.7: Error graph for top-oil temperature of substation 2

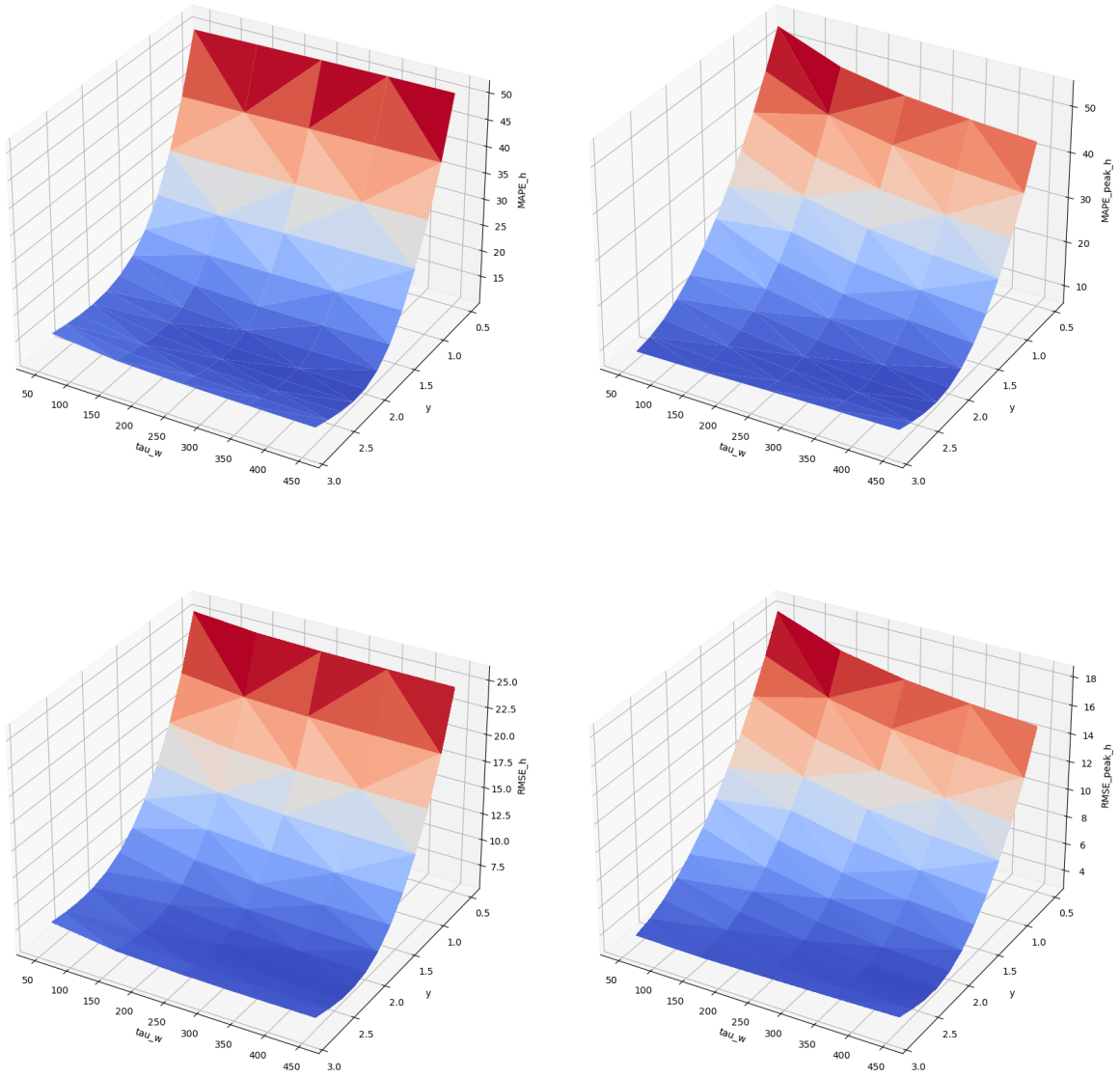

Figure B.8: Error graph for hot-spot temperature of substation 2

B.3. Substation 3

In this case, the simulated top-oil temperatures in figure B.9 show large reactions to reductions in load factor. Furthermore, the cyclic thermal behaviour of the simulated top-oil temperature seemed to have a lower axis than that of the measured top-oil temperature. Similar behaviour was observed in the simulated hot-spot temperature.

To reduce the reaction to load changes, the oil time constant τ_o is increased. Furthermore, to raise the axis of the cyclic behaviour, the oil exponent x is reduced. These changes resulted in the thermal behaviour shown in figure B.10.

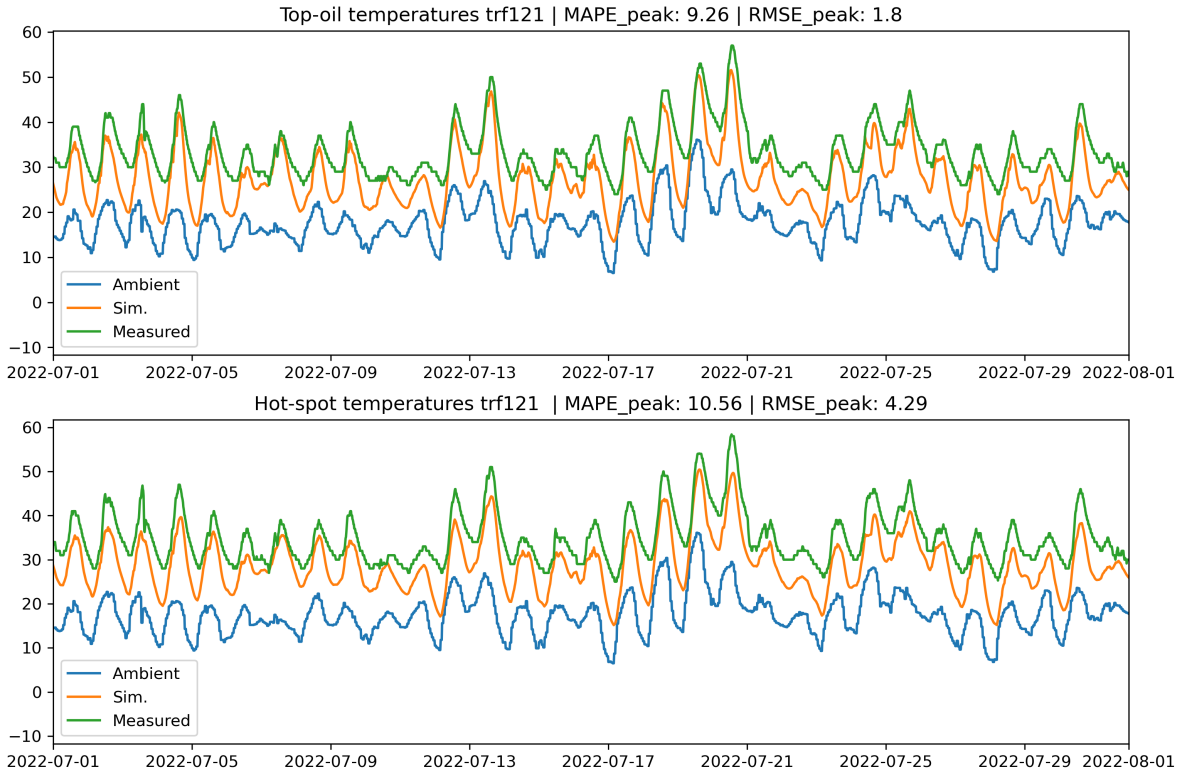

Figure B.9: Curve fitted model temperature behaviour of substation 3

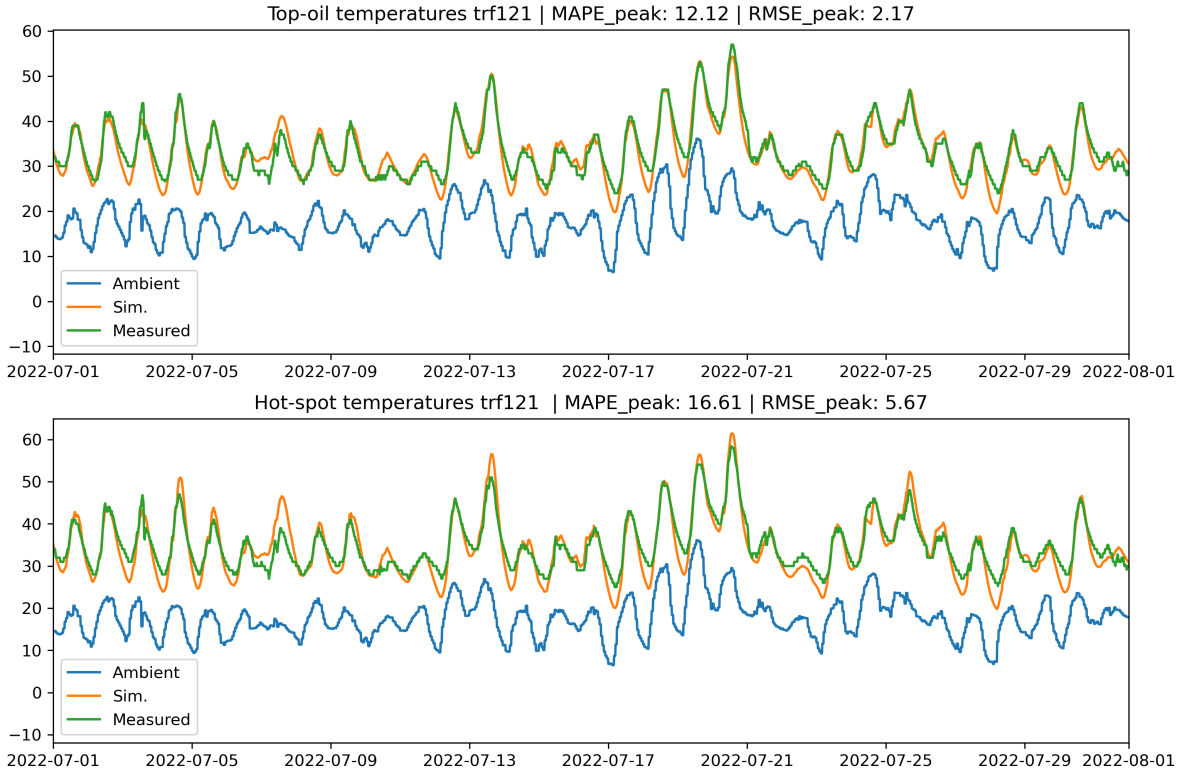

Figure B.10: Manually fitted model temperature behaviour of substation 3

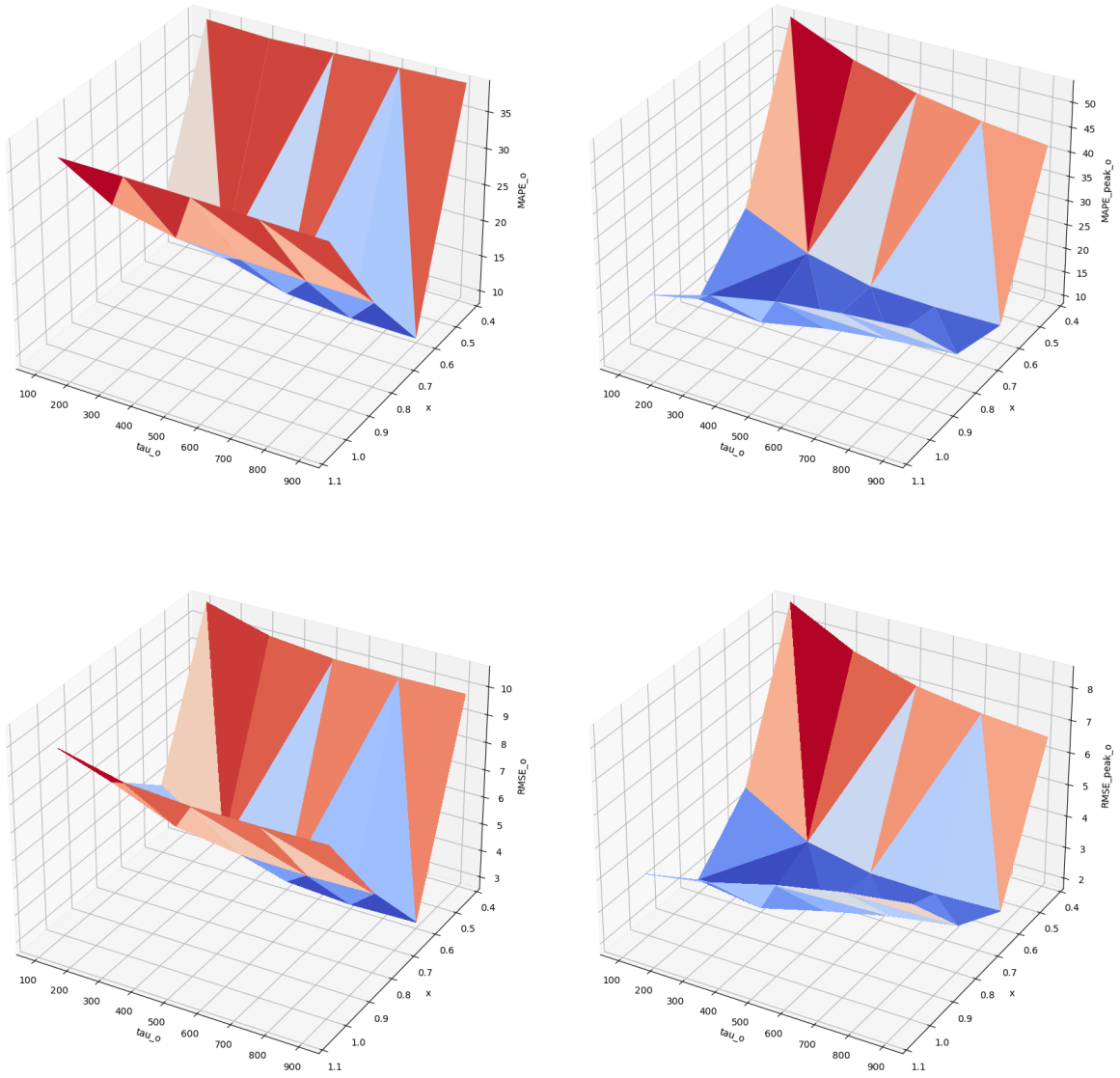

Figure B.11: Error graph for top-oil temperature of substation 3

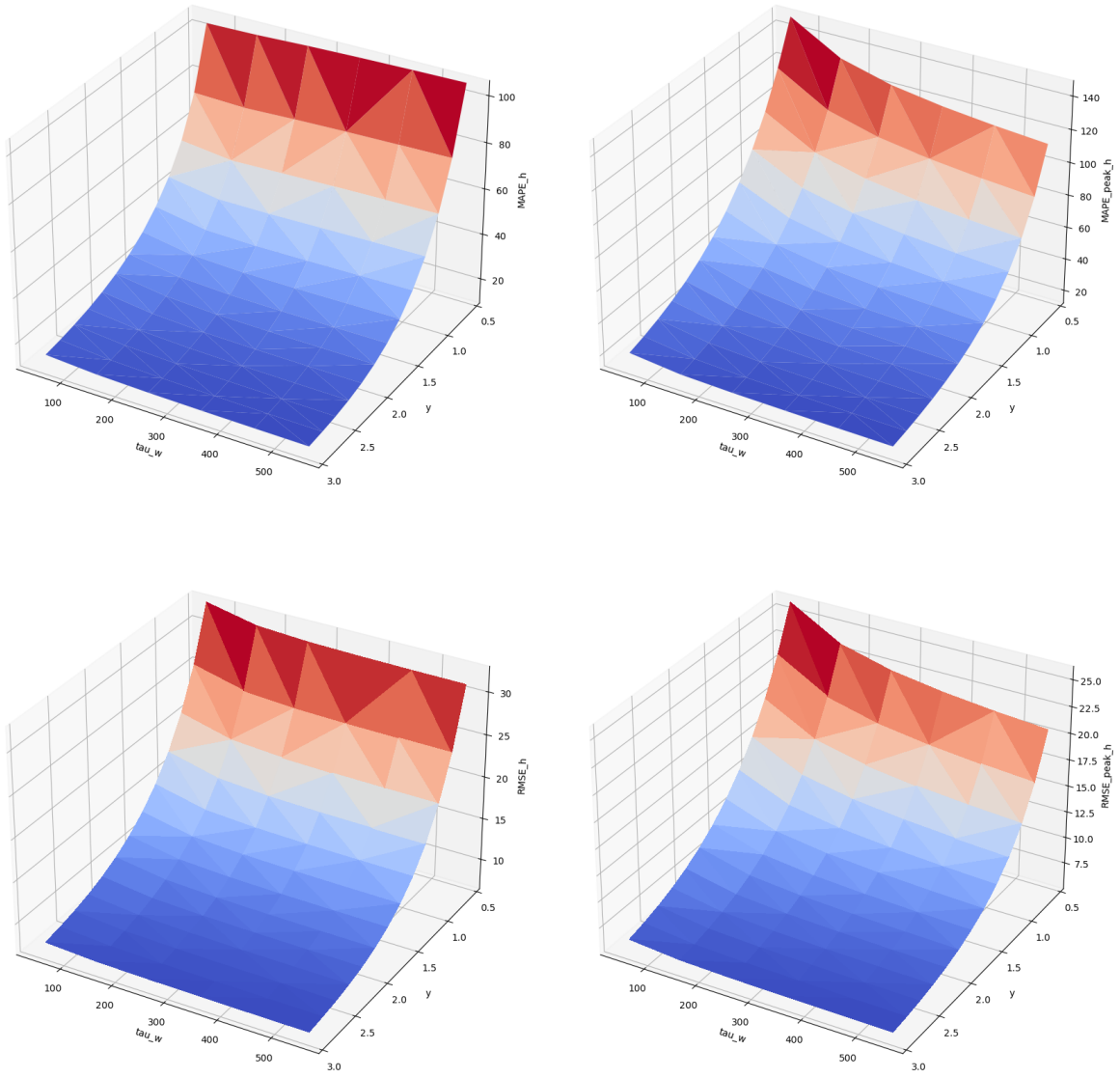

Figure B.12: Error graph for hot-spot temperature of substation 3

B.4. Substation 4

The curve fitted model of substation 4's base case show undershoot of both the simulated top-oil and hot-spot temperature, as can be seen in figure B.13. By reducing the oil and winding time constants, the model shows overshoot of the simulated top-oil and hot-spot temperatures, as can be seen in figure B.14.

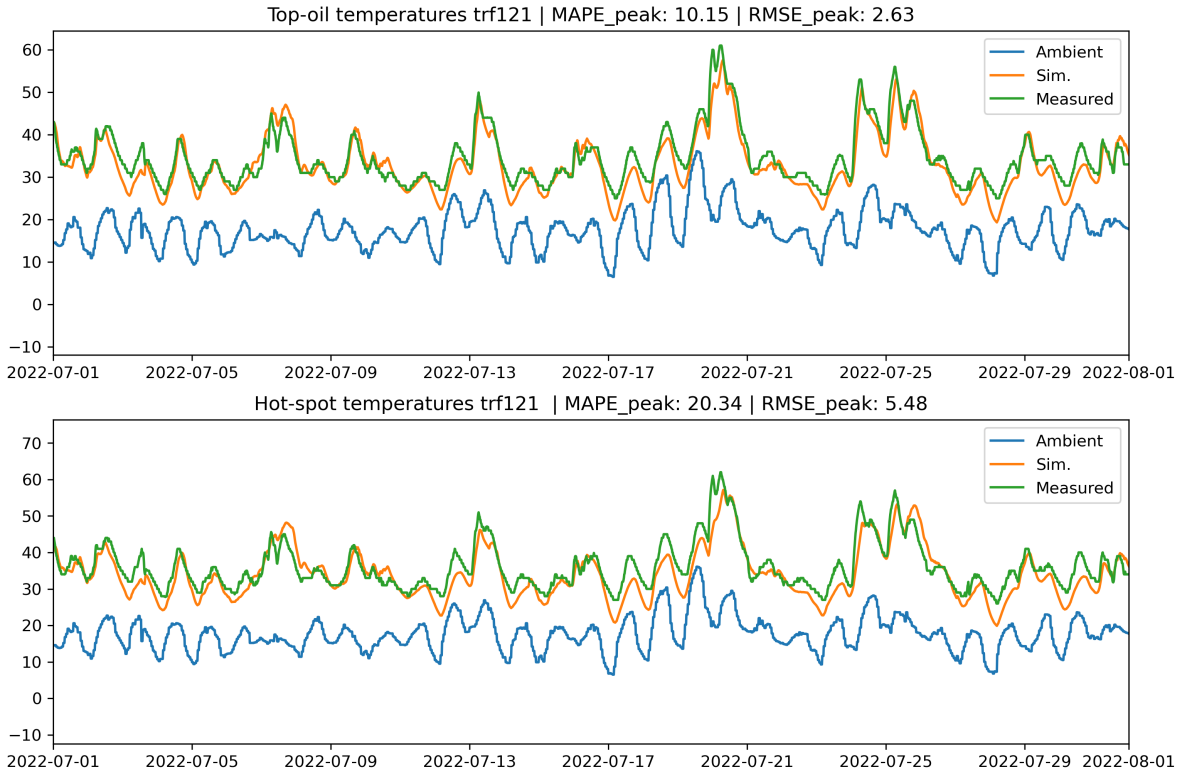

Figure B.13: Curve fitted model temperature behaviour of substation 4

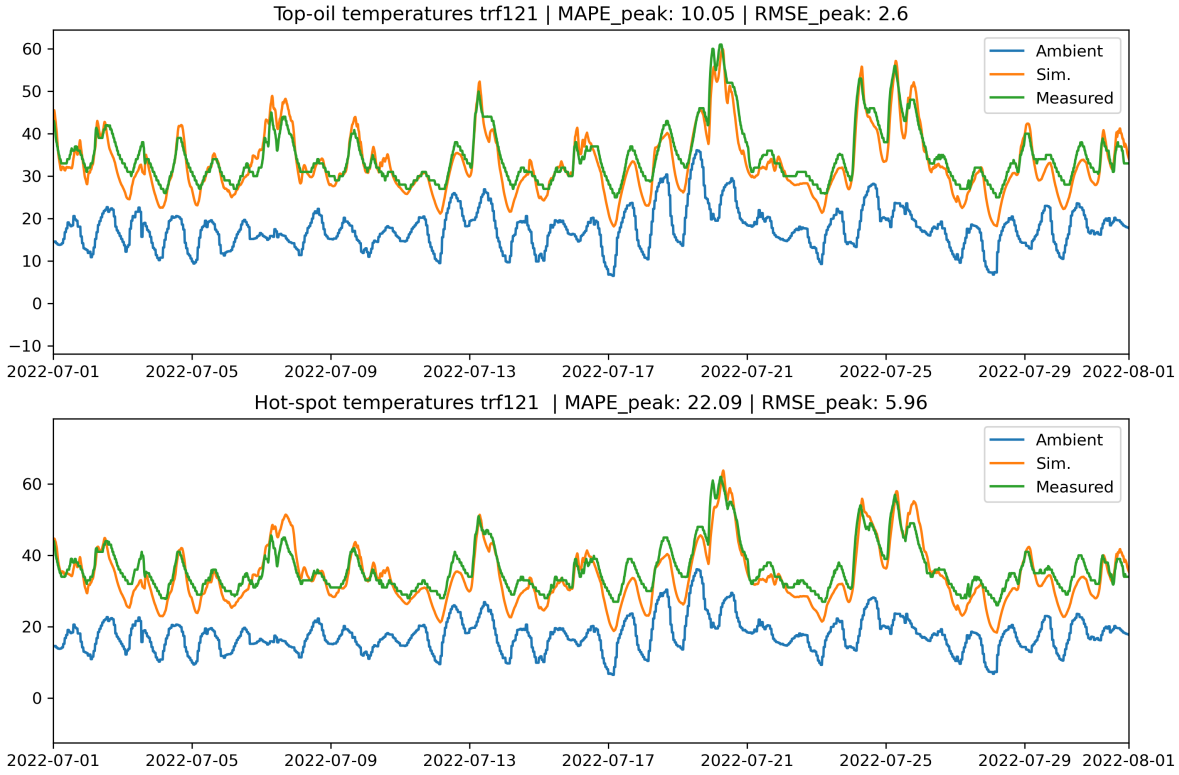

Figure B.14: Manually fitted model temperature behaviour of substation 4

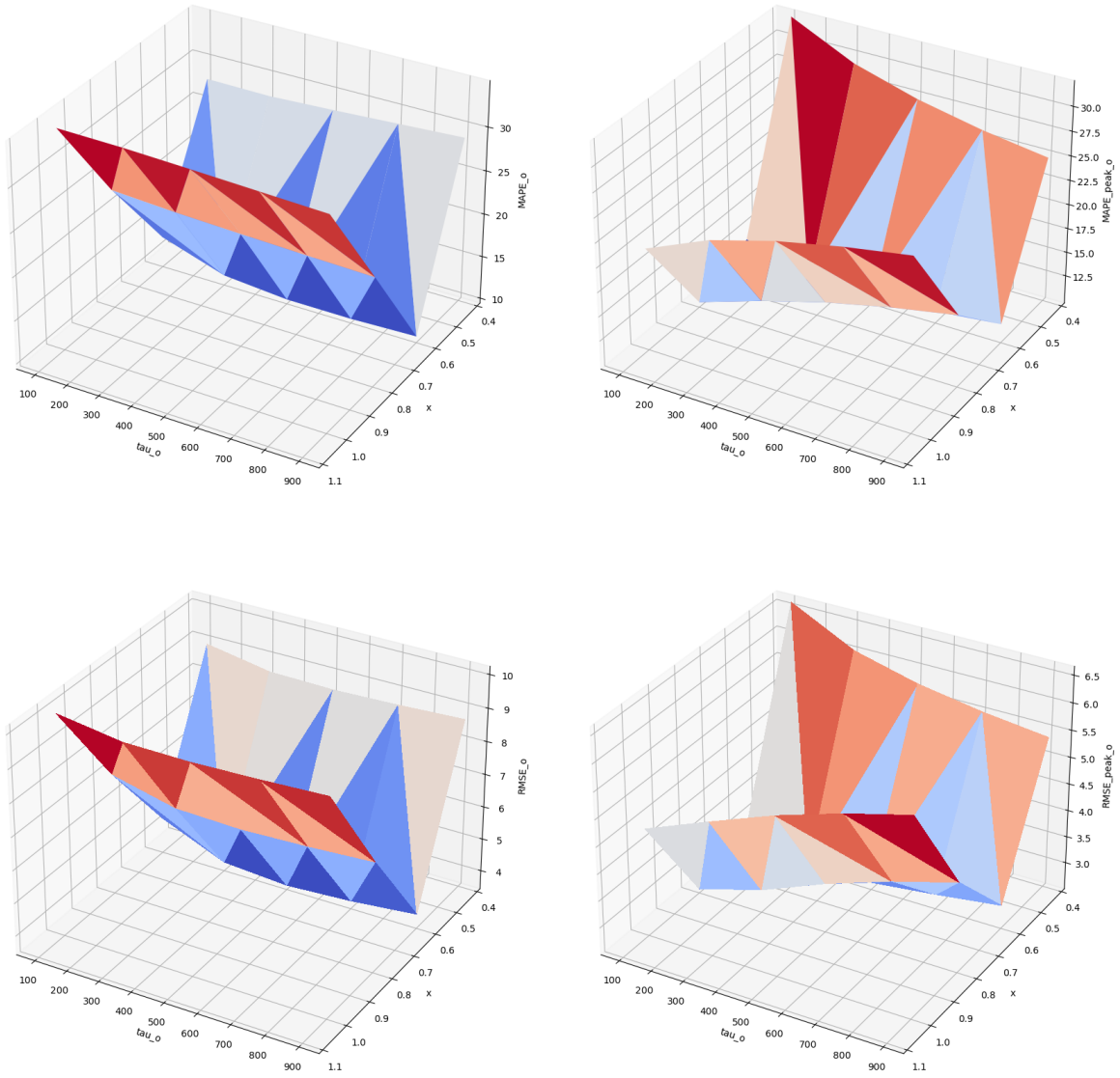

Figure B.15: Error graph for top-oil temperature of substation 4

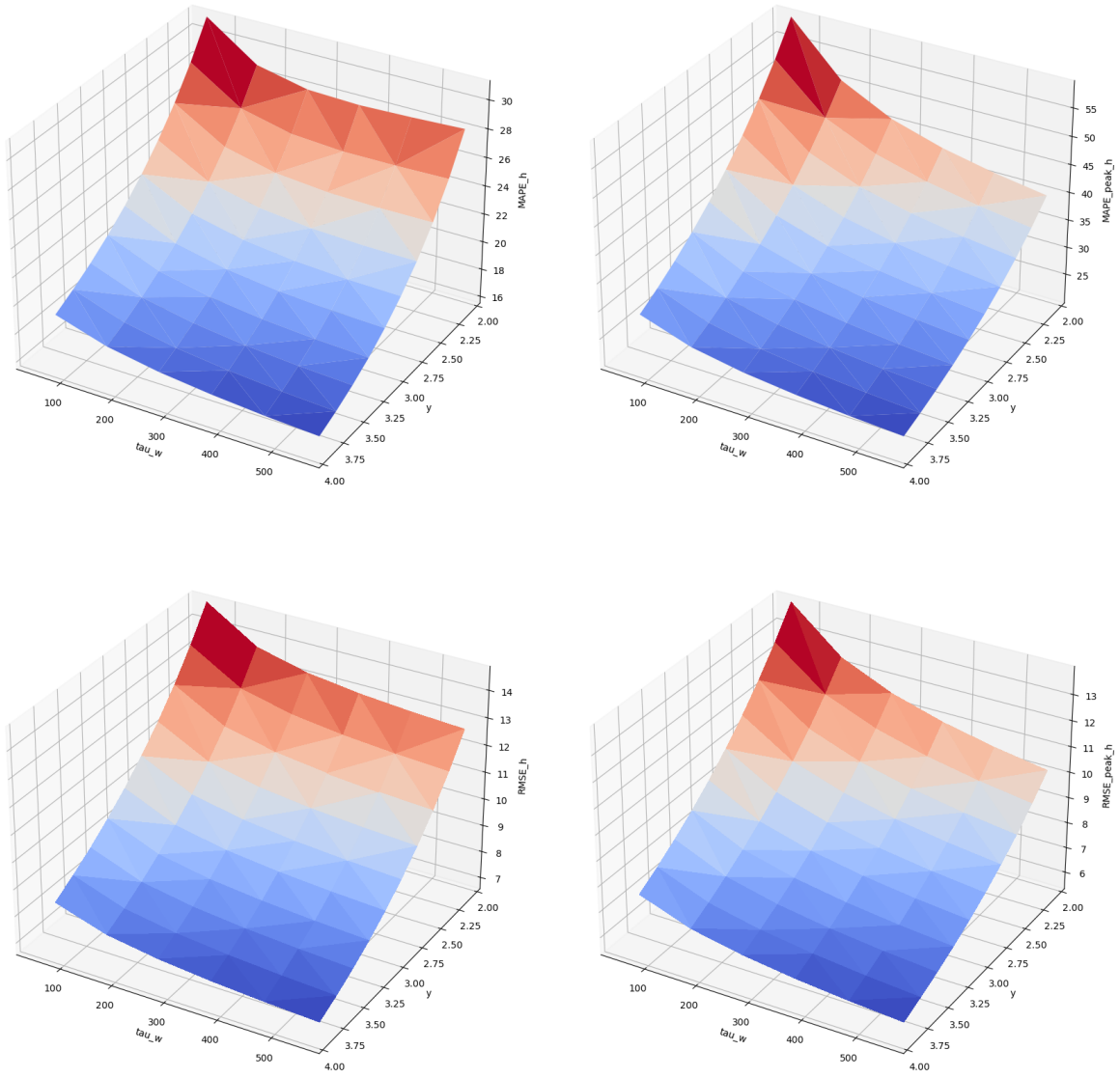

Figure B.16: Error graph for hot-spot temperature of substation 4